HHS Public Access

Author manuscript

Biomaterials. Author manuscript; available in PMC 2021 March 01.

Published in final edited form as:

Biomaterials. 2020 March ; 233: 119750. doi:10.1016/j.biomaterials.2019.119750.

Investigational New Drug enabling angiotensin oral-delivery studies to attenuate pulmonary hypertension

Henry Daniell[1,*], **Venkata Mangu**[1], **Bakhtiyor Yakubov**[2], **Jiyoung Park**[1], **Peyman Habibi**[1], **Yao Shi**[1], **Patricia A. Gonnella**[1], **Amanda Fisher**[2], **Todd Cook**[3], **Lily Zeng**[4], **Steven M. Kawut**[5], **Tim Lahm**[2,3,4]

[1]Department of Basic and Translational Sciences, School of Dental Medicine, University of Pennsylvania, Philadelphia, PA, USA;

[2]Department of Medicine; Division of Pulmonary, Critical Care and Occupational Medicine;

[3]Department of Cellular and Integrative Physiology, Indiana University School of Medicine, Indianapolis IN, USA;

[4]Richard L. Roudebush VA Medical Center, Indianapolis, IN, USA;

[5]Department of Medicine, Perelman School of Medicine, University of Pennsylvania, Philadelphia, PA, USA.

Abstract

Pulmonary arterial hypertension (PAH) is a deadly and uncurable disease characterized by remodeling of the pulmonary vasculature and increased pulmonary artery pressure. Angiotensin Converting Enzyme 2 (ACE2) and its product, angiotensin-(1–7) were expressed in lettuce chloroplasts to facilitate affordable oral drug delivery. Lyophilized lettuce cells were stable up to 28 months at ambient temperature with proper folding, assembly of CTB-Ace2/Ang1–7 and functionality. When the antibiotic resistance gene was removed, Ang1–7 expression was stable in subsequent generations in marker-free transplastomic lines. oral gavage of monocrotaline-induced PAH rats resulted in dose-dependent delivery of Ang-(1–7) and ACE2 in plasma/tissues and PAH development was attenuated with decreases in right ventricular (RV) hypertrophy, RV systolic

[*]**Corresponding Author**: Dr. Henry Daniell, W.D. Miller Professor, Vice Chair, Department of Basic and Translational Sciences, School of Dental Medicine, University of Pennsylvania, Philadelphia PA 19104-6030. hdaniell@upenn.edu; Phone : (215) 746-2563.

Author contributions

HD conceived this project, designed experiments, interpreted data, participated in SMARTT study design/discussions and wrote/edited several versions of this manuscript. VM created and characterized CTB-Ang1-7 plants (with or without marker) and wrote these sections. YS and PH evaluated biomass and expression level in some of the batches of plants grown at Fraunhofer or the greenhouse. JP contributed data on CTB-ACE 2 characterization and wrote related text. BY generated and analyzed PAH data, AF generated hemodynamic data, TC generated echocardiography data, LZ helped in data analysis and TL designed PAH experimental studies, performed data analysis and wrote PAH sections of this manuscript. SMK wrote clinical design section and participated in SMARTT study design and discussions.

Conflict of Interest

There is no specific financial conflict to disclose. All authors have declared that no conflict of interest exists to report.

The authors declare that they have no known competing financial interests or personal relationships that could have appeared to influence the work reported in this paper.

pressure, total pulmonary resistance and pulmonary artery remodeling. Such attenuation correlated well with alterations in the transcription of Ang-(1–7) receptor MAS and angiotensin II receptor AGTRI as well as IL-1β and TGF-β1. Toxicology studies showed that both male and female rats tolerated ~10-fold ACE2/Ang-(1–7) higher than efficacy dose. Plant cell wall degrading enzymes enhanced plasma levels of orally delivered protein drug bioencapsulated within plant cells. Efficient attenuation of PAH with no toxicity augurs well for clinical advancement of the first oral protein therapy to prevent/treat underlying pathology for this disease.

Graphical Abstract

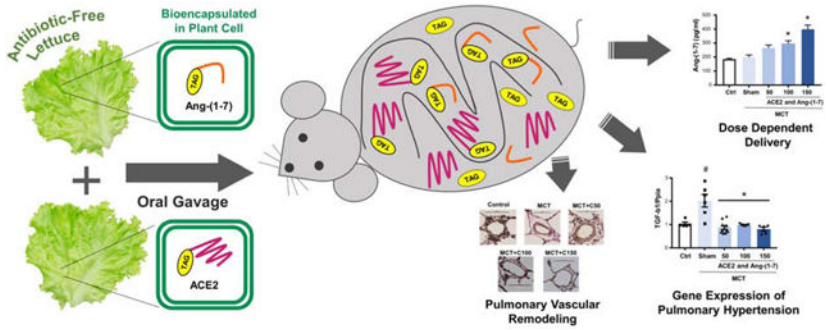

Keywords

Affordable drug delivery; chloroplast; pharmacokinetics; toxicology; storage

Introduction

Fifty years ago, recombinant human insulin was made in yeast or bacteria and injections save millions of lives. Despite WHO listing insulin as an “essential priority medicine” it is not affordable for >90% of global population. Insulin pumps cost $6000–12,000 but one third of the global population earn <$2 per day. Death of American citizens due to unaffordability of insulin (NPR September 1, 2018, January 4 CBS 2019) underscores this problem even in the US, where price of insulin has doubled in the past five years. Indeed, the cost of the top 10 biologic drugs currently sold exceeds 75% GDP of all countries. Therefore, exploring alternate methods of production and delivery of affordable protein drugs is an urgent unmet medical need.

Among several hurdles for delivering protein drugs (PD) orally, the first challenge is to get PDs protected from digestion by stomach enzymes or acids. The second challenge is their release from the protective covering of PDs (bioencapsulated) in the gut lumen. The third challenge is penetration of the gut epithelial cells to reach the circulatory system. All these three challenges are addressed when PDs are expressed within plant cells. Plant cell walls have β 1,4 and β 1,6 linkages, which are not hydrolyzed by human or animal digestive enzymes. Therefore, plant cell wall protects PDs from acids and enzymes in the stomach. When intact plant cells reach the gut, commensal bacteria release enzymes that breakdown β 1,4 and β 1,6 linkages in the plant cell wall and PDs are released in the gut lumen [1–3]. When cell penetrating peptides are fused to protein drugs, they cross the gut epithelium and

are delivered into plasma [1–3]. Utilizing this delivery system, several protein drugs have been delivered orally to treat diabetes [4, 5], pulmonary hypertension [6], Alzheimer's disease [7], retinopathy [8], and hemophilia [9–12], in small or large animal disease models. Oral drug delivery is especially suitable for treatment of diseases that require daily injections and long-term treatments. In addition to enhancing patient compliance, the cost of PDs is reduced by elimination of expensive fermentation and purification processes that are used to make current biopharmaceuticals [1–3]. Storage of PDs in lyophilized plant cells at ambient temperature for many years without losing their efficacy further reduces their cost by elimination of cold storage and transportation [1–3, 11–13].

Pulmonary arterial hypertension (PAH) is a deadly disease resulting in elevated pulmonary vascular resistance and pulmonary artery pressure, characterized by remodeling of the pulmonary vasculature, [14]. Smooth muscle hypertrophy, endothelial proliferation, and adventitial thickening in the small pulmonary arteries lead to increased right ventricular (RV) afterload with RV dysfunction, failure, and death. This is of critical importance, as the long-term treatment of PAH currently is limited by expense (ranging from $60K to > $100,000-$200,000 / year per patient), frequent side effects and suboptimal survival of only 55% at 3 years [15]. The latter is due at least in part to a lack of effect of currently available drugs on pulmonary vascular remodeling [14, 16–18]. In addition, short half-life of current drugs (small molecules) require continuous or frequent intravenous delivery [19].

The renin-angiotensin-aldosterone system (RAAS) plays important roles in regulation of several physiology and pathogenesis signaling pathways, especially in the cardiovascular system [20]. In the RAAS, Angiotensin-Converting Enzyme (ACE) converts Angiotensin I (Ang I) to Angiotensin II (Ang II), and Ang II stimulates the AT1 receptor (AT1R). On the other hand, Angiotensin-Converting Enzyme 2 (ACE2), a homolog to ACE, produces angiotensin-(1–7) [Ang-(1–7)] from Ang II, which leads to activation of the Mas receptor. The ACE2/Ang-(1–7)/Mas axis has protective effects in the heart, blood vessels, kidney and central nervous system, acting as a homeostatic regulator of vascular function by counteracting the ACE/AngII/AT1R axis [21]. Importantly, PAH is characterized by significant up-regulation of the RAAS [22–24]. In fact, several pre-clinical and clinical studies suggest that RAAS inhibition may prevent PAH development and attenuate severity [25–30]. Recent studies identified a protective role of the ACE2/Ang-(1–7)/Mas axis in animal models of PAH [6, 31–36]. While these studies demonstrated that activation of ACE2 or Ang-(1–7) signaling is beneficial in animal models of PAH and pulmonary hypertension (PH) due to lung fibrosis, oral delivery systems for repetitive delivery of ACE2/Ang-(1–7) are not available, thus limiting their clinical applicability.

In this study, expression level of ACE2 was enhanced through codon optimization and clinical grade materials were produced in a cGMP facility. Both ACE2 and Ang1–7 were expressed in lettuce chloroplasts and Ang1–7 plants free of antibiotic resistance genes were evaluated for stability of expression in subsequent generations. Pharmacokinetics, pharmacodynamics, safety, toxicology and tolerability studies of orally delivered ACE2/ Ang-(1–7) bioencapsulated in plant cells were conducted. Prevention and treatment of underlying pathology of PAH through oral delivery of ACE2/Ang-(1–7) should facilitate

regulatory approval, clinical studies, and affordable convenient oral protein drug for treatment of pulmonary hypertension.

RESULTS

Codon optimization of the human ACE2 gene

To increase expression level of the native human ACE2 gene, codon optimization was carried out. Codon usage database as a reference was built based on translation codons of the most highly expressed gene in chloroplasts, *psbA*, from 133 plant species [11, 37]. Out of 805 amino acid codons of the native ACE2, 481 codons, including 59 rare codons were replaced, changing the coding sequence AT content from 57 % to 62% (Supp. Table. S2). It should be noted that codons were not replaced with those used at highest frequency in the psbA gene because it reduced translation due to limited tRNA pools (data not shown). Therefore, the codon usage hierarchy of the most highly expressed chloroplast gene (psbA) was used in this optimization process.

Generation of CTB-ACE2 lettuce transplastomic lines

Native CTB (Cholera non-Toxin B subunit) was fused to human ACE2 codon optimized sequence or the native human Ang-(1–7) sequence. Ang-(1–7) sequence didn't require codon optimization because the native sequence was expressed at high levels in tobacco [6]. In between CTB and ACE2 or Ang-(1–7), a hinge region (Gly, Pro, Gly, Pro) followed by furin cleavage site (Arg, Arg, Lys, Arg, Ser, Val; [38]) was inserted to prevent any steric hindrance. The furin cleavage site facilitates release of ACE2 or Ang-(1–7) from CTB and furin is an ubiquitous protease present in all human cell types [5]. In the chloroplast expression cassette, CTB-ACE2 or CTB-Ang-(1–7) is regulated by the strong psbA promoter and 5' UTR (Fig. 1A) and the psbA 3' UTR enhances transcript stability. CTB-ACE2 and Ang-(1–7) plasmids containing expression cassettes were then delivered into the lettuce chloroplasts by biolistic particle delivery system and the transplastomic plants were screened and confirmed by genomic DNA PCR or Southern blot analysis (Fig. 1 B and C).

PCR amplifications using three primer sets annealing the flanking regions of the cassette (16s-F/aadA-R, UTR-F/23s-R) and internal regions (CTB-F/UTR-R) confirmed site specific integration of the CTB-ACE2 expression cassette (Fig. 1B). Southern blot analysis of *Hind*III digested CTB-ACE2 genomic DNA showed 10 kb and 3.7 kb hybridizing fragments in transplastomic lines of lettuce chloroplast genome but a single 9.1 kb fragment was observed in untransformed lines. Absence of the 9.1 kb fragment in transplastomic lines confirms their homoplasmic state and therefore the CTB-ACE2 cassette is present in all copies of chloroplast genome in transplastomic lines (Fig. 1C).

Generation of CTB-Ang-(1–7) marker-free lettuce transplastomic lines

A schematic diagram for generation of marker-free transplastomic lines is shown in Suppl. Fig. S1. The CTB-Ang-(1–7) DNA sequence was cloned into the marker-free lettuce chloroplast transformation vector pLS-MF (Fig. 1D). The expression cassette of the CTB-Ang-(1–7) is identical to CTB-ACE 2 except the insertion of two direct repeat sequences. To eliminate selectable marker (aadA) gene in transplastomic plants, the aminoglycoside-3'-

adenylyl-transferase gene (aadA), was inserted between two direct repeats of chloroplast encoded CF1 ATPase β subunit (atpB) gene non-coding sequence. The site-specific integration of the CTB-Ang-(1–7) transgenes cassette into the chloroplast genome was examined using PCR. The primers that anneal to the native 16s rRNA gene flanking the transgene cassette and the aadA selectable marker gene yielded specific 3.3 kb product in all the evaluated transplastomic lines (Suppl. Fig S2A). Likewise, amplification using primers that anneal to the atpB region and 16s rRNA gene sequence generated 2.4 kb product, and 3'UTR and 23s rRNA gene primers generated 2.4 kb product in all the selected transformants (Suppl. Fig S2A), while no PCR product was observed in untransformed plants. To further evaluate homoplasmic nature of transplastomic lines, total plant gDNA was digested with *Hin*d III and probed with the DIG-labeled trnI and trnA flanking sequence [11]. All the transplastomic lines showed 12.6 kb hybridizing fragment (with the marker gene), while there was no untransformed wild type fragment at 9.1 kb. Absence of 9.1 kb fragment in transplastomic lines confirmed homoplasmy of the CTB-Ang-(1–7) lines (Suppl. Fig 2B). In addition, all the transplastomic lines showed additional 10.6 kb size hybridization fragment, suggesting partial excision of the aadA gene (Suppl. Fig 2B).

Because homologous recombination takes place between the two directly repeated atpB sequences, this should eventually lead to excision of the selectable marker gene (aadA) cassette in transplastomic lines. Therefore, seeds from T0 homoplasmic lines seeds germinated on half-strength MS medium (Suppl. Table S3). After a week, spectinomycin resistant and sensitive plants were observed (Suppl. Fig. S3; Suppl. Table. S3). The pale-yellow shoots recovered to normal green color when transferred to ½ MS0 medium in the absence of spectinomycin and recovered plants confirmed loss of the transgene cassette based on PCR analysis (data not shown). In the second strategy, leaf samples from some of the T1 progeny of parent line #6 containing both maker and marker-free plastid genomes (Suppl. Table S3) was sub-cultured on shoot induction medium and regenerated plants were screened. The PCR results showed that most of the pale-yellow color shoots were marker-free (Suppl. Fig. 1E). To further evaluate homoplasmic nature of selectable marker-free transplastomic lines, total plant gDNA was digested with *Hin*dIII and probed with the DIG-labeled trnI and trnA flanking sequence [11]. Four marker-free transplastomic lines showed 10.6 kb fragment, compared to two transplastomic plants with marker gene showed 12.6 kb fragment size, while there was no untransformed wild type fragment at 9.1 kb. Absence of 9.1 kb fragment in transplastomic lines confirmed homoplasmy of the CTB-Ang-(1–7) lines (Fig. 1F). The pale-yellow color shoots (Suppl. Fig. S4D) were further sub cultured on MS-shoot induction medium without spectinomycin. The selectable marker-gene elimination in 28 out of 48 shoots was confirmed by PCR (Suppl. Fig 5 A, B, C). To further confirm stability of excision of the aadA gene, total plant gDNA extracted from selectable marker-free plants was digested with Hind III and probed with the DIG-labeled trnI and trnA flanking region [11]. Two transplastomic lines showed 12.6 kb fragment (with the marker gene), four transplastomic lines showed 10.6 kb (without marker gene), while there was no untransformed wild type fragment at 9.1 kb. Absence of 9.1 kb fragment in transplastomic lines confirmed the homoplasmy of CTB-Ang-(1–7) plants (Suppl. Fig 5 D, E). The selectable marker-free plants were transferred to the greenhouse and seeds were collected. The removal of the aadA gene was further re-confirmed by germination assays (Suppl. Fig.

S6) and molecular analysis (Fig. 3 A, B). Western blot analysis showed no significant difference in expression of CTB-Ang1–7 in marker-free plants and those with the antibiotic resistance gene (Fig. 3C).

Increased expression of codon optimized ACE2

CTB-ACE2 expression levels in transplastomic plants were compared between the native human Ace2 or codon optimized Ace2 genes in western blots (Fig. 2A). When relative intensities of ACE2 proteins were compared using RbCL (endogenous chloroplast protein) as a loading control, codon optimized gene (1.59 ± 0.7) was ~100-fold higher (P = 0.002) than the native human gene (0.015 ± 0.006). However, when ACE2 protein was quantified using the CTB standard loaded in the same blot, ACE2 (N) line was 0.15 (± 0.005) ug/mg and ACE2 (co) line was 6.49 (± 0.43) ug/mg, with 42.7 fold increase after codon optimization (P = 0.003). The native human gene product ACE2(N) showed multiple peptides and smear on the blot due to incomplete synthesis and poor translation efficiency, while codon optimized product CTB-ACE2(co) showed a clear single ~101 kDa protein (Fig 2A).

Characterization of CTB-ACE2 (co) in lyophilized lettuce

Functionality of CTB was confirmed via GM1 receptor ELISA assay after lyophilization (Fig. 2E). For prolonged storage at ambient temperature, the transplastomic leaves were lyophilized as described previously [11, 37]. Proper folding of CTB in a pentameric form allows it bind to GM1 receptor located in gut epithelial cells, which facilitates CTB-ACE2 to cross the gut epithelium and enter into the circulatory system, where CTB is released from ACE2 through furin cleavage [1]. Absorbance value at 450 nm against GM1 receptor of CTB-ACE2(co) in fresh and lyophilized plants was performed (Fig. 2B). CTB-ACE2(co) in fresh plant showed the proper folding, assembly and disulfide bonds. Lyophilized plant cells stored for 3 months showed proper folding and assembly of the CTB pentamer structures, for efficient GM1 receptor binding, similar to CTB control. In addition, stability of CTB-Ace2 after long-term storage (1–28 months) at ambient temperature was evaluated in lyophilized cells stored up to 28 months for toxicology, 4 months for pharmacokinetic and 1–11 months for PAH studies (Table S1).

Characterization of CTB-Ang-(1–7) in lyophilized lettuce

Western blot analysis showed a fusion protein of 12.4 kDa in 6 different next generation transplastomic lines (T1), with no cross-reacting proteins from untransformed plants, when probed with CTB antibody (Fig. 2C, D). In further analysis, a significant difference in CTB-Ang-(1–7) intensity was observed with equal loading of proteins (equal weight) from fresh or lyophilized plant cells, in a serial dilution (Fig. 2D). For evaluation of stability of fusion protein in long term storage, leaves harvested from fully grown lettuce were lyophilized as described in the previous studies [11, 13]. Homoplasmic CTB-Ang-(1–7) formed pentamers and showed binding affinity to the GM1-ganglioside receptor through ELISA assays (Fig. 2E). The stability of CTB-Ang1–7 after long-term storage of lyophilized cells at ambient temperature for 20 months for toxicology, 7–8 months for pharmacokinetic and 9–20 months for PAH studies (Table S1)). These results confirm proper folding, assembly, disulfide bonds and stability of CTB-Ang-(1–7) pentameric structure in lyophilized lettuce leaves.

Clinical grade and scale-up production of CTB-ACE2 (co) and CTB-Ang-(1–7)

Transplastomic lettuce expressing CTB-ACE2 (co) was grown in a Fraunhofer hydroponic facility, as described previously [13]. Plants were harvested on 47, 66, 82, 106 days and CTB-ACE2 (co) (Fig. 2F, 2G) expression level, and biomass per plant (Fig 2H) were quantified and compared with plants grown in the greenhouse (30, 46,60, 82 days). Compared to the greenhouse, the expression level of CTB-ACE2 from the hydroponic system showed higher level; however, the biomass per plant was 10 times less than greenhouse. The highest amount of protein level (8.6 mg/g DW) was obtained in the hydroponic system in 106 days after sowing; however; this batch showed lowest biomass per plants. Moreover, CTB-ACE2(co) expressions in three different transplastomic lines (#1, #2, and #3) were evaluated by western blots after long term storage at ambient temperature from 6 months to 12 months (Fig. 2I). Percentage of CTB-ACE2(co) expression levels in total protein (TP) was compared between the percentage evaluated in a month after lyophilization (0 m) and the one after different storage durations, 6, 10, and 12 months. No significant differences (P-value > 0.1 vs. 0 month by ANOVA) in ACE2 levels were observed in lyophilized lettuce plant cells stored for 12 months at ambient temperature. Expression level of CTB-Ang-(1–7) was in plants with or without the selectable marker gene and expression was stable in subsequent generations after removal of the antibiotic resistance gene (Fig 3C, D). Expression level of CTB-Ang1–7 was very low on 46 days in the hydroponic system when biomass yield was the highest (Fig. 3F). Beyond 46 days biomass yield steadily decreased and reached the lowest level when CTB-Ang1–7 level expression was the highest. In contrast, greenhouse grown plants yielded steady levels of biomass per plant and maintained similar levels of expression (Fig 3F).

Pharmacokinetic study of orally delivered CTB-ACE2 and CTB-Ang-(1–7)

To investigate the effects of bioencapsulated CTB-ACE2 and CTB-Ang-(1–7) in a model of PAH, we performed oral gavage of CTB-ACE2 and CTB-Ang-(1–7) in rats with monocrotaline (MCT)-induced PH, daily five times weekly for four weeks. Lyophilized plant cells were suspended in PBS and given at the following doses: 1.5, 3, and 4.5 mg/kg of CTB-Ang-(1–7) and 1, 1.75, and 2.3 mg/kg of CTB-ACE2. These doses are based on previous studies using CTB-Ace2 and CTB-Ang1–7 expressed in tobacco cells that resulted in successful attenuation of PAH [6]. The goal of the combination studies was not to achieve equal dose of Ang-(1–7) and ACE2 because both provide the same drug (Ang1–7) directly or through the action of Ace2 by cleaving angiotensin. Previous investigations [6] revealed that both proteins offered better efficacy in attenuation of PAH than either one alone. Because of differences in expression levels in different batches of harvest or growth, uniform drug dose was administered in all studies by using corresponding dry weight of lyophilized cells (Table S1). Increase in circulating Ang-(1–7) plasma levels were dose dependent (Fig.4 A–E). The highest levels were achieved with the highest CTB-ACE2 and CTB-Ang-(1–7) dose in the fourth week, confirming dose-dependent drug delivery. Pooled sera samples show statistically reliable delivery of Ang1–7 to plasma at medium and high dose. However, when data was plotted with individual mice data at different duration (1–4 weeks), statistical reliability is observed at all ages in the highest dose. Drug delivery was done to simulate clinical conditions rather than optimal measurement conditions by withdrawal of food [39].

In a limited number of animals (n=3–6/group), we measured lung ACE2 activity and Ang-(1–7) levels and both ACE2 and Ang-(1–7) levels increased based on dose delivered. Interestingly, PH development was associated with a significant decrease in lung ACE2 levels. Lung Ang-(1,7) levels did not decrease with PH development, but increased with CTB-ACE2 and CTB-Ang-(1–7) oral delivery (Fig. 4 F–H). Lung Ang1–7 and Ace2 were ~10-fold higher than plasma levels. Lung Ace2 activity was dose dependent except that at the highest dosage digestion of plant cells may be a limitation (Fig 4F). However, lung Ace2 and Ang1–7 levels were not dose dependent. Plasma levels and tissue levels of Ang-(1–7) do not correlate due to release of Ang-(1–7) into exosomes as discussed later, with Ang-(1–7) therefore not being captured in plasma measurements. In addition, lack of correlation is also due to analysis of whole lung tissues rather than measurements specifically in pulmonary vascular cells. However, both ACE2 and Ang-(1–7) levels either increased significantly or tended to increase.

Plant cell walls have β 1,4 and β 1,6 linkages, which are not hydrolyzed by human digestive enzymes. Intact plant cells therefore protect protein drugs from acid hydrolysis and digestive enzymes in the stomach [1]. However, plant cell wall should be digested by enzymes that cleave β 1,4 and β 1,6 linkages. This is naturally done by cellulolytic bacteria present in the gut. By simulating action of gut bacteria, we fed mice first with a mixture of plant cells expressing pectinase, mannanase, endoglucanase and exoglucanase [39], followed by protein drug (IGF1) bioencapsulated in plant cells. Mice fed with plant cell wall degrading enzymes increased concentration of IGF1 in the plasma, confirming that plant cell wall digestion is important for enhancing protein drug delivery (Figure 4I). This confirms protection of the protein drug in the stomach from acids/enzymes and release in the gut lumen by the action of cell wall degrading enzymes in the gut lumen and enhanced absorption.

Attenuation of MCT-PH by oral delivery of bioencapsulated ACE2 and Ang-(1–7)

We next evaluated the effects of bioencapsulated CTB-ACE2 and CTB-Ang-(1–7) on PH endpoints. Oral delivery of ACE2/Ang-(1–7) resulted in attenuation of PH development, evidenced by 30–50% decreases in RV hypertrophy, RV systolic pressure (RVSP), total pulmonary resistance index and pulmonary artery (PA) remodeling compared to sham animals (Fig. 5A, B, D, E). The most consistent effects were noted with 100 mg (1.75/3 mg/kg) of bioencapsulated CTB-ACE2 and CTB-Ang-(1–7), followed by the 150 mg (2.3/4.5 mg/kg) dose.

Cardiac index tended to increase with ACE2/Ang-(1–7) but failed to reach statistical significance (Fig. 5C). The lack of a decrease in cardiac index is a limitation of our studies. Systemic blood pressure (measured invasively as mean arterial pressure) and heart rate were not affected by MCT or ACE2/Ang-(1–7) (Suppl. Fig. S7). MCT administration may have led to RV abnormalities that are not captured by cardiac index at rest and under general anesthesia (e.g. RV-pulmonary artery uncoupling or diastolic dysfunction). We observed a ~20% mortality in the MCT group, which may have led to survival bias, with relatively maintained cardiac index values in the surviving animals. However, MCT-induced changes in RVSP, RV hypertrophy and pulmonary artery remodeling were robust, indicating that MCT indeed induced a robust PH phenotype. Drug delivery was well-tolerated and there

was no difference in weight curves between animals gavaged with CTB-ACE2/CTB-Ang-(1–7) *vs.* sham animals (Suppl. Fig. S7).

RAAS signaling alteration and pulmonary vascular remodeling by oral delivery of bioencapsulated ACE2 and Ang-(1–7)

In the next step, we assessed effects of bioencapsulated CTB-ACE2 and CTB-Ang-(1–7) on expression of genes implicated in RAAS signaling and/or PAH pathogenesis. We first evaluated mRNA expression of the Ang-(1–7) receptor Mas1. Mas 1 level increased 2-fold after PH development in the sham group but were similar to healthy control animals after CTB-ACE2 and CTB-Ang-(1–7) feeding (Fig. 6A). A similar pattern was noted when we measured mRNA for the angiotensin II receptor AGTR1 (Fig. 6B). The mRNA of IL-1β, a pro-inflammatory cytokine implicated in PAH pathogenesis, was elevated 2-fold after MCT, whereas CTB-ACE2 and CTB-Ang-(1–7) administration was associated with a dose-dependent decrease in IL-1β mRNA abundance as compared to the untreated MCT group (Fig. 6C). A similar pattern was noted for IL-1β receptor 1 but failed to reach statistical significance (Fig. 6D). Lastly, CTB-ACE2 and CTB-Ang-(1–7) attenuated PH-induced increases in mRNA expression of TGF-β1, a growth factor that is a major driver of PAH development and PA remodelg [40, 41] (Fig. 6E). Taken together, these data indicate that combinational feeding with bioencapsulated CTB-ACE2 and CTB-Ang-(1–7) attenuates PH-induced alterations in expression of genes implicated in neurohormonal signaling, inflammation and pulmonary vascular remodeling. The mRNA was extracted from whole lung homogenates. We speculate that many of the changes observed are happening in the pulmonary vasculature but are aware that whole lung homogenates capture changes in all the various cell types and compartments of the lung. We have noted this as a limitation and are planning to perform localization studies (e.g., FiSH) and studies in isolated pulmonary artery endothelial cells and smooth muscle cells in the future. Inhibition studies, for example with a MAS inhibitor, would be interesting indeed in order to determine that effects of CTB-ACE2 and CTB-Ang-(1–7) indeed are mediated by MAS receptor activation. We are planning to perform such studies in the future (using pharmacologic inhibitors and knockdown/knockout approaches) and have included a statement regarding this in the revised manuscript.

Lack of observable toxicity upon oral delivery of CTB-ACE2/Ang-(1–7)

Oral dose range finding (DRF) studies of CTB-ACE2/CTB-Ang-(1–7) in healthy male and female Sprague Dawley rats were done at SRI. Third party performance of toxicology studies was set up by the NIH NHLBI SMARTT program. Animals were included into one of three groups with escalating dose ranges: low dose (Group-I), medium dose (Group-II), and high dose (Group-III) containing ACE2–0.08/Ang-(1–7)-1.72, ACE2–0.4/Ang-(1–7)-8.6, and ACE2–0.8/Ang-(1–7)-17.2 mg/kg rat body weight with negative controls (Group-0). All animals survived until their scheduled sacrifice although slight and moderate squinting eyes were observed in all males and females, in Group-III on Day 1 (Suppl. Table S4). All females in Group-III showed moderate discharge on both eyes and were slightly hypoactive after dose on Day 1 but returned to normal the next day. All other groups were normal throughout the study.

Individual animal body weight was monitored (Suppl. Table S5 and Suppl. Fig. S8). Males in Group-III (high dose) showed a slight decrease in body weight on Days 3 and 8. There was a slight body weight loss in the females of Group-III on Days 1–3, but it returned to normal by Day 8. In hematology evaluations (Suppl. Table S6), slight, but statistically significant, increases in hematocrit (HCT) and absolute reticulocytes (ARET) were observed in males of Group-III (high dose) on Day 3 (by 15% and 13%, respectively). In Groups-II (mid dose) and III (high dose), a slight, but statistically significant, increase in percent lymphocytes (PLY) was observed on Day 3 (by 10% and 8%, respectively). Neutrophils (absolute count and percent) were decreased in the test material-treated males when compared with the control group. In females, a slight, but statistically significant, decrease in percent basophils (PBA) was observed in Group-III (high dose) on Day 3 (by 38%). These changes were slight and within the normal historical range and are considered to be of minimal toxicological significance according to SRI toxicology report.

Effects of oral administration of CTB-ACE2/CTB-Ang-(1–7) on clinical chemistry were also evaluated (Suppl. Table S7). A slight, but statistically significant, increase (18%) in albumin (ALB) was observed in the males of Group-III (high dose) on Day 3. Slight increases in sodium (SOD) and chloride (CHL) were also observed in the males of test material-treated groups compared with respective controls. No increases in creatinine or ALT were noted in any animal. In fact, in females, slight decreases in these parameters were observed in test article-treated groups when compared with respective controls. These changes were slight, sporadic, and within the normal historical range, and therefore are considered to be of minimal toxicological significance. Necropsy revealed only insignificant minor changes that are considered to be of minimal toxicological significance (Suppl. Table S8), according to SRI toxicology report.

Single dose pharmacokinetic study of orally delivered CTB-ACE2 and CTB-Ang-(1–7)

Pharmacokinetics studies of CTB-ACE2/Ang-(1–7) were performed after a single oral gavage with three different doses to healthy Sprague Dawley rats at SRI. Third party performance of pharmacokinetic studies was set up by the NIH NHLBI SMARTT program. The dosage was defined as low (Group-I), medium (Group-II), and high (Group-III); these contain ACE2–0.25/Ang-(1–7)-4.2, ACE2–0.5/Ang-(1–7)-8.5, and ACE2–1/Ang-(1–7)-17 mg/kg rat body weight, respectively. Group I (low dose) showed a time dependent ACE 2 activity in plasma. It is interesting to note that ACE2 activities in sera are maintained from 15 minutes to 48 hours in this group (data not shown). There was no significant difference in ACE2 activity in plasma between female and male rats in all three groups in any of the detection time points. After feeding a single dose in mice, lower increase in Ace2 was observed in plasma but higher accumulation was observed in different tissues as shown in Figure 4. Single dose studies were not as conclusive as repeat dose studies described above.

Design of clinical studies

The next step for this potential therapeutic is a “first in man” Phase I study in healthy volunteers to evaluate the safety/tolerability and pharmacodynamics and pharmacokinetics of oral bioencapsulated ACE2/Ang-(1–7). The aims of this study would be to determine the maximum tolerated dose of ACE2/Ang-(1–7), to evaluate the rate and extent of absorption

of ACE2/Ang-(1–7), to understand the clearance mechanisms and metabolites of ACE2/Ang-(1–7), and to characterize the safety profile of orally administered ACE2/Ang-(1–7) across a range of doses. The main endpoints of this study will be safety and tolerability, including symptoms, vital signs (including systemic blood pressure), and clinical laboratories. Pharmacokinetic endpoints, including RAAS Equilibrium Analysis will be included. Pharmacodynamic analysis would include assessment of Ang-(1–7) and Ang-(1–5) by LC/MS. Dose-escalation by cohort will occur with the initial dose determined by our pre-clinical studies. There will be predetermined stopping rules and a Safety Review Committee will meet after each cohort's data are complete before proceeding to the next cohort. Single dose administration of ACE2/Ang-(1–7) will occur in four cohorts each with four weeks of observation. An additional cohort will receive the maximal tolerated dose of ACE2/Ang-(1–7) orally administered twice per day for seven days.

DISCUSSION

PAH is a progressive and fatal disease characterized by remodeling of the pulmonary vasculature, resulting in elevated pulmonary vascular resistance and increased PA pressure. There clearly is an unmet need for a potent oral therapy for PAH, distinct in mechanism from other treatments, which improves the survival in this universally fatal and incurable disease [17, 18]. There is no current therapy to prevent PAH or treat the underlying pathology, although current drugs help to manage symptoms of PAH. In order to address these concerns, we first expressed the native human ACE2 and Ang-(1–7) genes, fused with the transmucosal carrier CTB in tobacco chloroplasts and orally delivered these drugs as frozen plant powder in rats with MCT-induced PH. Both proteins were protected in the stomach from acids and enzymes by the plant cell wall but commensal bacteria digested cell wall and released them in the gut lumen. CTB bound to GM1 receptors and delivered both ACE2 and Ang-(1–7) to plasma. Oral delivery significantly improved cardio-pulmonary structure and functions in rats with MCT-induced PH in both prevention and reversal protocols [6]. The RVSP significantly decreased and the pulmonary blood flow was improved. Therefore, oral ACE2/Ang-(1–7) feeding improved RV function and attenuated maladaptive remodeling in diseased animals [6].

The first challenge to advance this concept to the clinic is to achieve higher level expression of ACE2 in an edible chloroplast system because tobacco is not an acceptable system for FDA approval. Chloroplast is an ideal bioreactor for high level expression of prokaryotic genes [42] (>50% TSP) or smaller human proteins like proinsulin (22.5 kDa, >70% TSP [43,44]. However, large proteins such as CTB fused human coagulation factor IX, 59.2 kDa (0.56% TSP), and CTB-coagulation factor VIII heavy chain (FVIII-HC), 86.4 kDa (0.05% TSP) were poorly expressed [11, 13, 37]. In order to address this challenge, Daniell lab has developed new software to optimize codons and enhance expression of large human blood proteins [11, 37]. In the current study, CTB-ACE2 (101.1 kDa) was codon optimized and its expression level was increased up to 100-fold when compared to the CTB-ACE2 native human gene. The native human gene expression resulted in a ladder with a number of cleaved proteins whereas codon optimizations enhanced stability and expression level, without any observable degraded proteins in western blots.

Utilizing the high-level expression transplastomic lines, we produced clinical grade material in Fraunhofer cGMP facility for our efficacy, toxicology and pharmacokinetic studies. CTB-ACE2(co) is stable in lyophilized lettuce cells up to 28 months when stored at ambient temperature. This is remarkable advantage of this cGMP production platform and facilitates the low-cost production and transportation of ACE2 totally eliminating cold storage. Yield of biomass with optimal expression of Ace2/Ang1–7 is important in order to reduce the amount of plant powder packaged in each capsule. Therefore, transplastomic lettuce expressing both protein drugs were grown in the Fraunhofer hydroponic facility and compared with natural growth conditions in the Daniell lab greenhouse. CTB-Ang1–7 greenhouse grown plants yielded ten times more biomass per plant and maintained optimal levels of expression throughout the growth cycle, facilitating multiple rounds of biomass harvest. However, in the Fraunhofer hydroponic system, CTB-Ang1–7 was very low when biomass yield was the highest in the first harvest and highest expression of CTB-Ang1–7 was observed in the last harvest when biomass yield was the lowest. Sixty CTB-Ang1–7 greenhouse-grown plants produced 214.41g expressing 1.32–1.53 mg/g DW, whereas 800 hydroponically-grown plants produced 452.17g expressing 1.45–1.94 mg/g DW, with a 6 -7-fold difference in yield of the protein drug per plant. Expression level of CTB-ACE2 from the hydroponic system showed a similar pattern with ten times lower biomass per plant than the greenhouse (0.26 Vs 2.27 DW per plant). Similar pattern of biomass and yield of foreign protein was observed for enzymes produced in transplastomic plants [45,46]. Reasons for these include overcrowding of plants in the hydroponic facility designed to save space. In addition, LED lights provided 70–90 μmol/m^2/s intensity, whereas greenhouse natural sun light provided 280–300 μmol/m^2/s intensity. Plants were grown at Fraunhofer in 18h light/6 h dark whereas it was 16h light/8h dark, providing 2 hours of additional light. Temperature cycle at Fraunhofer was set at 25°C± 1°C, whereas in the greenhouse it was set at 22°C±1°C in the day and 20°C±1°C at night. Therefore, further optimization of growth conditions at Fraunhofer is required to increase yield of biomass and protein drug for commercial scale production.

The next major challenge in regulatory approval is the presence of the antibiotic resistance gene, which is needed for selection of cells expressing ACE2/Ang-(1–7). Spectinomycin specifically binds to chloroplast ribosomes and blocks protein synthesis. Therefore, plant cells without the transgene cassette containing the aadA gene are bleached but only those with stably integrated transgene cassette will produce green shoots. Therefore, the selectable marker gene is essential to create transplastomic lines. However, after confirmation of stable integration of foreign genes, the antibiotic resistance gene is no longer required, and its continued presence increases the metabolic load by making a foreign protein that is no longer needed. Removal of the antibiotic resistance gene reduces the metabolic load and also facilitates reuse of the same antibiotic resistance marker for subsequent transformation events. Although FDA has approved use of antibiotic resistance genes in genetically modified food crops consumed in the past three decades, European regulatory agencies have required their removal. In this study, we removed the aadA gene from the inverted repeat region of the lettuce chloroplast genome using direct repeat sequences flanking the aadA gene and utilizing the chloroplast homologous recombination system. Previous studies have shown that direct DNA repeats >600 bp promote homology-based marker excision in

tobacco chloroplast genomes from the single copy region [47, 48]. However, it is more challenging to remove the selectable marker gene when transgenes are integrated into the inverted repeat of the chloroplast genome, due to the copy correction mechanism that maintains identical inverted repeat regions (including spacer regions) found in >800 sequenced chloroplast genomes [49]. Daniell lab recently developed the first application of marker-free transplastomic lettuce expressing food/feed enzymes [45,46]. In these studies, the *aadA* gene was successfully excised even in the first round of selection. However, in this study, we demonstrate that the selectable marker gene can be removed from CTB-Ang1–7 lines at several stages during plant transformation or even after obtaining seeds in the next generation. In addition, we show that generation of maker-free transplastomic edible plants is efficient and numerous lines can be obtained after germination of seedlings. We achieved complete deletion of the antibiotic resistance gene (*aadA*) and observed stable maintenance of CTB-Ang1–7 in the next generation. Expression level of CTB-Ang-(1–7) in plants with or without the selectable marker gene was the same and stable in subsequent generations after removal of the antibiotic resistance gene.

Neurohormonal imbalance with increased RAAS activation is accepted as an important disease mediator in PAH [22–24]. Robust evidence from experimental and clinical studies suggests that RAAS inhibition may prevent PAH development and attenuate severity [25–30]. While the role of renin, angiotensin and aldosterone has been studied in PAH for more than one decade, recent studies have identified a protective role of the ACE2/Ang-(1–7)-Mas axis [6, 31–36]. While these studies demonstrated that activation of ACE2 or Ang-(1–7) signaling is meritorious in animal models of PAH and PH due to lung fibrosis, oral delivery systems for repetitive delivery of ACE2/Ang-(1–7) are not available, thus limiting their clinical applicability.

Strengths of our PAH studies include the robust and progressive PH model with high mortality, the investigation of dose responses, the detailed hemodynamic, structural and biochemical/molecular phenotyping, and the study of Ang-(1–7) plasma levels over several time points. Since ACE2 mediates Ang-(1–7) production, we measured Ang-(1–7) plasma levels as a read-out for effectiveness of ACE2 and Ang-(1–7) delivery. We noted an increase in Ang-(1–7) levels with higher doses of plant cells, suggesting that digestion of plant cells by commensal bacteria is not a major limitation. Although plasma levels were twice as high as in unfed controls, tissue levels were ten-fold higher. Our studies therefore suggest that a doubling in plasma levels of Ang-(1–7) is sufficient to attenuate PH development. Furthermore, we did not note any difference in levels between different experimental batches, again suggesting consistent and reliable drug delivery. It should be noted that we administered the plant material once/day rather than twice/day as done in a previous study [6]. Efficacy of a single dose would be expected to be helpful in clinical trial design and patient compliance.

Interestingly, plasma Ang-(1–7) levels in the MCT-PH model did not fully correlate with effects on PH endpoints. For example, despite a lack of a statistically significant increase in Ang-(1–7) plasma levels, the lower dose of plant material exhibited significant effects on MCT-PH endpoints (albeit slightly less consistent than the two higher doses). The highest plasma levels were reached with the 150 mg (2.3/4.5 mg/kg) dose of bioencapsulated CTB-

ACE2 and CTB-Ang-(1–7), whereas the most consistent effects on MCT-PH endpoints were observed with the 100 mg (1.75/3 mg/kg) dose. Since levels of Ang-(1–7) and Ace2 measured in lung were 10 times higher than plasma levels, a potential explanation for these findings could be that tissue levels of Ang-(1–7) do not correlate with plasma levels. For example, in mice fed with a single oral gavage of CTB-ACE2 lettuce, there was only a moderate increase in serum ACE2 activities, however the tissue ACE2 activities were significantly increased. This may be because we used full-length human ACE2 protein in this study, which includes a transmembrane binding domain [50]. In human clinical trials, a soluble form of truncated recombinant ACE2 has been used, deleting the transmembrane domain [51]. However, this needs further investigation because elevated ACE2 activity in plasma represents loss of the protective effect but elevated tissue level leads to protective effect [52]. Similar trend was observed in diabetic nephropathy where elevated ACE2 levels in plasma had no beneficial effect [53]. Therefore, future studies could compare the effect of full length ACE2 or without the transmembrane domain or include exosome profiling for comparative evaluation of plasma and tissue ACE2 levels during treatment.

Numerous examples show that protein drugs can be reproducibly delivered in small (rat, mice) or large (dog) animals, irrespective of their diet or location in the US, suggesting that species or geographic variability in gut microbes do not significantly influence oral drug delivery. However, this doesn't mean that microbes capable of digesting plant cells are abundant in the gut mucosa. Despite numerous studies on gut microbiome [54], very little is known about their unique functions. Very few studies have tested the small intestine microbiota in humans, where most digestion and absorption occur. Duodenal microbiota is abundant in firmicutes that are capable of digesting plant cells [55]. Past duodenum, there is less digestion but more absorption. One approach would be to enrich gut microbes using probiotics but so far these approaches have not yet been successful. In this study, we tested a much simpler and direct approach by expressing plant wall degrading enzymes [45, 46]. We recently showed that a mixture of mannanase, pectinate lyase, endoglucanase, exoglucanase released protein drugs *in vitro* by co-incubation with cells expressing enzymes [39]. These enzymes facilitate hydrolysis of α and β 1,4 linkages of mannan (hemicellulose), pectin, and cellulose respectively, which are three major components of plant cell wall [56]. In this study, sequential oral feeding of plant cell wall degrading enzymes followed by plant cells expressing a protein drug increased concentration of the drug in plasma (*p=0.009). These studies may have profound impact on enhancing release and absorption of protein drugs bioencapsulated in plant cells. In addition, release of more nutrients/vitamins from plant cells could help address malnutrition challenges.

Bioencapsulated CTB-ACE2 and CTB-Ang-(1–7) attenuated expression of mRNA of several genes that have been strongly linked to PAH pathogenesis. TGF-β is a major driver of proliferative and fibrotic processes in the pulmonary vasculature and has been identified as a major contributor to pulmonary vascular remodeling [40, 41]. The decrease in TGF-β 1 mRNA noted with CTB-ACE2/CTB-Ang-(1–7) suggests that this growth factor is either directly regulated by ACE2 and/or Ang-(1–7), or that its decrease is secondary to ACE2/Ang-(1–7) effects on upstream regulators of TGF-β. Similarly, IL-1 β has been identified as a significant promoter of PAH development [57], and its decrease (as well as the strong trend for a decrease in expression of IL-1 β receptor 1) with CTB-ACE2/CTB-Ang-(1–7)

indicates that this could be a direct or indirect target of ACE2/Ang-(1–7). The finding of decreased pulmonary vascular remodeling is in line with strong antiproliferative properties of Ang-(1–7) demonstrated in vascular smooth muscle cells and cancer cells [58, 59].

The decrease in mRNA for the angiotensin II receptor AGTR1 after CTB-ACE2/CTB-Ang-(1–7) was of particular interest. Since ACE2 and Ang-(1–7) are RAAS inhibitors, this could indicate that there indeed was less RAAS activation with CTB-ACE2/CTB-Ang-(1–7) treatment. Ang-(1–7) signals through the G protein-coupled receptor Mas1. The concurrent decrease in Mas1 expression was somewhat surprising but may be a consequence of Ang-(1–7) administration and subsequent down-regulation of receptor expression. With more Ang-(1–7) in the system, up-regulation of Mas1 (as seen in MCT rats receiving PBS only) may not be necessary to inhibit RAAS activation. It was surprising that both TGF-β 1 and AGTR1 mRNA levels decreased by all three doses of plant cells expressing CTB-Ace2 and CRB-Ang1–7, whereas total pulmonary resistance and PA remodeling were only affected by the two higher doses. This suggests that repression of these genes is not sufficient to attenuate pulmonary vascular remodeling and that additional genes including IL-1 β (which was only decreased by the two higher doses of plant material), need to be repressed as well in order for ACE2/Ang-(1–7) to attenuate this endpoint.

The objective of this dose range-finding (DRF) toxicity study conducted at SRI was to determine potential toxicity of mixed test agents, Ls-CTB-ACE2 and Ls-CTB-ANG (1–7), fusion proteins expressed in lettuce chloroplasts, in adult male and female Sprague Dawley rats following twice per day (b.i.d.) oral administration. Information from this study may be used to determine dose levels for subsequent toxicity studies and the suitability of the proposed human dose. Male and female Sprague Dawley rats (3/sex/group) were given b.i.d oral dose of Ls-CTB-ACE2/Ls-CTB-Ang-(1–7) combination at 0.08/1.7, 0.4/8.6 or 0.8/17 mg/kg total. Animals were sacrificed on Day 8 and evaluated for mortality/morbidity, clinical observations, body weights, clinical pathology (hematology and serum chemistry), and gross necropsy observation. According to SRI toxicology report “All animals survived until their scheduled sacrifice. No drug-related effects were observed for clinical observations, body weights, clinical pathology, and gross necropsy observations”. In conclusion, male and female Sprague Dawley rats tolerated a b.i.d. oral administration of Ls-CTB-ACE2/Ls-CTB-Ang-(1–7) expressed in lettuce plant for a single day. Based on the toxicology parameters evaluated in this study, the MTD of Ls-CTB-ACE2/Ls-CTB-Ang-(1–7) in combination is believed to be slightly greater than 0.8/17 mg/kg Ls-CTB-ACE2/Ls-CTB-Ang-(1–7) when administered b.i.d. oral dose in rats. The NOAEL is considered to be 0.4/8.6 mg/kg Ls-CTB-ACE2/Ls-CTB-Ang-(1–7) (equivalent to plant material 500/500 mg/kg) in combination for a day of b.i.d. oral dose administration in rats.

In this study, we use ACE2 and Ang1–7 which are already present in the human plasma, but their dose should be carefully regulated. No foreign protein is introduced in this study. CTB is used as a transmucosal carrier but it is degraded and not detected in blood [60]. CTB is FDA approved protein drug and has been used in the clinic for several decades. Several studies show that CTB fusion proteins suppress antibody formation when orally delivered, making this an ideal fusion protein for protein drug delivery [1–13]. The drug dose of 0.2 mg/kg ACE2 was tested in human clinical studies based on safety data obtained with 0.4

mg/kg dose escalation studies [61]. In another human clinical study using healthy subjects, 100–1,200 ug/kg single dose recombinant ACE2 caused a dose dependent increase in Ang-(1–7) with lower dose (100–200 μg/kg) and remained unchanged in higher doses (400–1,200 μg/kg). This suggests that the amount of available angiotensin II may limit ACE2-mediated conversion to Ang-(1–7). Repeated dosing of ACE2 (400 μg/kg) caused minimal accumulation of ACE2 in plasma but Ang1–8 levels were suppressed during the entire period [62]. In our study, doses used in toxicology studies ranged from ACE2–0.08/Ang-(1–7)-1.7 to ACE2–0.8/Ang-(1–7)-17 mg/kg. The most efficacious dose for attenuation of PAH endpoints were 1.75/3 and 2.3/4.5 mg/kg of CTB-ACE2 and CTB-Ang-(1,7), respectively.

Enhancing expression levels through codon-optimization, the ability to grow therapeutic proteins expressing lettuce plants in a cGMP FDA-approved facility, the lack of potential toxicity of combined CTB-ACE2 and CTB-Ang-(1–7) expressed in lettuce chloroplast following oral administrations twice a day (BID) for 8 days, the stability of ACE2 activity in plasma for up to 48 hours and the ability for dose-dependent delivery of Ang-(1–7) to plasma offer promising leads for further clinical studies. Together with their stability at ambient temperature for several months due to lyophilization, therapeutic proteins expressed in plants could significantly reduce dosing frequencies and simplify administration regimens compared to currently used PAH treatment drugs. Taken together, our data indicate that chloroplast-derived CTB-ACE2/CTB-Ang-(1–7) could be a novel oral treatment strategy for PAH. Future studies will focus on corroborating these results in rescue protocols, in alternative animal models of PAH and advancing Phase I clinical trials.

Materials and Methods

Codon optimization of ACE 2

Reference codon optimization table was created based on codon usage preference of psbA genes from 133 plant species in Daniell lab [37]. Native ACE2 sequence was analyzed using GeneQuest program of Lasergene and compared with the psbA-based codon table. Less than 5% of codon used in the reference was replaced and the ACE2 codon sequences were changed mimicking the hierarchy usage of the psbA genes based on the reference table. The codon optimized ACE2 was synthesized (GenScript Biotech, Piscataway Township, NJ).

Generation of CTB-ACE2(co) in pLS chloroplast vector

The synthesized ACE2(co) was PCR amplified with CTB using CTB-*Nde*I-F, 5′-GAATTCCATATGACACCTCAAAATATTACTGAT-3′; *psh*AI-ACE2-R, CAATACGACCAAAGTCTCTAGATTAGAAAGAAGTCTGTACGTCATCAGT primers and it was cloned into pLS vector between *Nde*I and *phs*AI restriction sites. The insertions of cloned fragments were confirmed by restriction digestion analysis and CTB-ACE2 expression was confirmed in *E. coli*. Sequence was confirmed and pLS-CTB-ACE2(co) plasmid vectors were extracted from TOP10 *E. coli* cells using PureYield™ plasmid Midiprep System (Promega, Madison, WI) and used for particle bombardment as previously described [63].

Generation of CTB-Ang-(1–7) in pLS-MF chloroplast vector

The CTB-Ang-(1–7) fusion gene (360 bp) was amplified by using pLD-CTB-Ang-(1–7) vector as template with CTB-*Nde*I-F,5′-GAATTCCATATGACACCTCAAAATATTACTGAT-3′; *psh*AI-Ang-(1–7)-R,5′-GATCGACATTCGTCTCAAGGATGAATATATACACG-3′primer including nucleotide sequence corresponding to 7 amino acids of Ang-(1–7) peptide and cloned into *Nde*I and *phs*AI restriction sites of pLS-MF vector. The inserted fragment was confirmed by restriction digestion analysis and CTB-Ang-(1–7) expression in *E. coli*. Sequence confirmed pLS-MF-CTB-Ang-(1–7) plasmid vector was extracted and used for particle bombardment.

Generation of transplastomic Lettuce

The pLS-CTB-ACE2 (co) or pLS-MF-CTB-Ang-(1–7) were transformed into 4-week-old lettuce (*Lactuca sativa*) leaves by particle bombardment [63]. The selection and regeneration of transplastomic lettuce plants were performed as described previously [11]. The homologous integration of CTB-ACE2(co) or pLS-MF-CTB-Ang-(1–7) genes into regenerated shoots were evaluated by PCR amplification and Southern blot analysis using specific primers sets and probes (Fig. 1A). The oligo nucleotide sequences of primers used for PCR analysis are 16s-F, 5′-CAGCAGCCGCGGTAATACAGAGGATGCAAGC-3′; aadA-R, 5′-CCGCGTTGTTTCATCAAGCCTTACGGTCACC; CTB-*Nde*I-F, 5′-GAATTCCATATGACACCTCAAAATATTACTGAT; trnA-R, 5’-CATTAGCTGTCCGCTCTCAGGTTGGGCAGT; atpB-R, 5’-GAATTAACCGATCGACGTGCTAGCGGACATT; UTR-F, 5′-AGGAGCAATAACGCCCTCTTGATAAAA C; 23s-R, 5′-TGCACCCCTACCTCCTTTATCACTGAGC. PCR positive plants were subjected one more round of selection. Total genomic DNA (2 μg) from untransformed and transgenic plants was digested with *Hind*III restriction enzymes and electrophoresed in 0.7% agarose gel. After depurination and denaturation, DNA was transferred to the nylon membrane (GE Healthcare life Sciences, Marlborough, MA). Southern blot analysis was performed to confirm the homoplasmic status of transplastomic lines by following the manufacture’s instruction of DIG high prime DNA labelling and detection starter kit II (Roche, Penzberg, Germany). The homoplasmic transgenic plants (3–5 leaf stage) were transferred to pots filled soil as described previously [11]. The next generation from ACE2 T1 seeds was hydroponically grown at Fraunhofer USA (Newark, DE) as previously described [13].

Total protein extraction and quantification of ACE2/Ang-(1–7)

After harvest from greenhouse and hydroponic growth, leaves were lyophilized and ground into fine powder as previously described [11]. Expression levels of CTB-ACE2 and CTB-Ang-(1–7) were quantified by western blots using CTB antibody and standards. Ten mg of lyophilized and ground plant power was rehydrated in 500 μl plant extraction buffer [11] for 1 hour at 4°C. The resuspended plant cells were sonicated in pulse on for 5 s and pulse off for 10 s, three times using sonicator 3000 (Misonix, Farmingdale, NY). After total proteins were quantified by Bradford assay (Bio-rad Laboratories, Hercules, CA), homogenized proteins were heated at 70°C in 1X Laemmli buffer for 15 min and run on SDS-polyacrylamide page (10 or 12 %). Western blot analysis was performed using anti-CTB

antibody (1:10000) (Gen Way Biotech, San Diego, CA) and goat anti rabbit IgG-HRP secondary antibody (1:4000) (Southern Biotechnology, Birmingham, AL). The precision plus protein standard was used as a standard (Bio-rad Laboratories, Hercules, CA). The proteins were detected by Supersignal west Pico Chemiluminescent substrate (Thermo Fisher Scientific, Waltham, MA) on to X-ray films, and then the proteins were quantified based on the intensities using ImageJ software (IJ 1.46; NIH). After the membrane was incubated in Western Stripping Buffer (Thermo Fisher Scientific, Waltham, MA) for 15 minutes at 37°C, western blot was performed against anti-RbcL (Agrisera, Vannas, Sweden) in PTM 1:40,000 for 1 hour for internal loading controls and then the subsequent western blot steps were followed as described above.

GM1-ganglioside receptor binding assay

To confirm ability of CTB-ACE2(co) or CTB-Ang-(1–7) expressed in lettuce cells to form pentamers binding to the GM1-ganglioside receptor, CTB-GM1 binding assay was performed. For GM1 binding assay, CTB-ACE2(co) or CTB-Ang-(1–7) protein was extracted from lyophilized plant by suspended in a ratio of 10 mg per 500 μl plant extraction buffer [11] and incubated for 1h at 4°C for rehydration. The buffer saturated lyophilized powder was sonicated (pulse on for 5s and pulse off for 10 s three times, using sonicator 3000, Misonix) and the supernatant was obtained by centrifuging at 12,000 rpm at 4°C for 5 min. CTB-ACE(co) or CTB-Ang-(1–7) GM1 binding assay was performed by following the protocol as described previously [11].

Excision of the antibiotic resistance gene in T1 seedlings

Seeds from self-pollinated flowers of T0 lines # 6 were collected and germinated on ½ MS0 medium containing 50 mg/L Spectinomycin. After a week, resistant seedlings showing green cotyledons and bleached yellow cotyledons were scored. The seedlings showing bleached phenotype were transferred to ½ MS0 medium without spectinomycin and recovered plant genotype was evaluated by PCR analysis. In addition, 3–4 weeks old T1 seedlings of T0 lines # 6 germinated on spectinomycin containing medium were cut into 0.5 cm size pieces and selected on shoot induction medium, supplemented with spectinomycin. The selectable marker elimination in regenerated shoots was analyzed by PCR and Southern blot analysis using specific primers sets and probes as described previously.

To reconfirm selectable marker gene elimination and stable inheritance of CTB-Ang-(1–7) gene in T1 generation, seeds from self-pollinated flowers of marker-free T0 plants were germinated on ½ MS0 medium containing 50 mg/L spectinomycin, along with T0 seeds containing the selectable marker-gene and untransformed wild type. After a couple of weeks spectinomycin resistance/spectinomycin sensitive phenotype was recorded. The selectable marker elimination in T1 seedlings was confirmed by PCR amplification and Southern blot analysis using specific primers sets and probes as described previously. CTB-Ang1–7 expression was confirmed by western blot analysis.

Animals and pharmacokinetic Study of CTB-ACE2 and CTB-Ang-(1–7)

Nine males and 9 females of Sprague Dawley rats were obtained from Charles River Laboratories (Hollister, CA). General procedures for animal care and housing were in

accordance with the current Association for Assessment and Accreditation of Laboratory Animal Care (AAALAC) recommendations, current requirements stated in the Guide for the Care and Use of Laboratory Animals (National Research Council), and current requirements as stated by the U.S. Department of Agriculture through the Animal Welfare Act and Animal Welfare Regulations (November 2013). Animals are assigned to test at the age of 10 weeks (males) and 12 weeks (females) at 250–325 g (males) and 200–275g (females) body weight range. The dosage was determined as low (Group-I), medium (Group-II), and high (Group-III), 3 males and 3 females in each group, which contain ACE2–0.125/Ang-(1–7)-2.1, ACE2–0.25/Ang-(1–7)-4.25, and ACE2–0.5/Ang-(1–7)-8.5 mg/kg rat body weight and they were orally administrated twice on Day1 Blood was collected from the JVC port into pre-chilled (~0 to −40 °C) tubes containing Heparin (Suppl. Table S1). Blood samples were centrifuged 30 min at 1,000 – 2,000 g using a refrigerated centrifuge. Plasma samples were then stored frozen at ≤ −60 °C. Collected blood volume was about 150 μl total whole blood (about 75 μl of plasma) per sample at pretest, 15, 30 min, 1, 2 4, 6, 24 and 48 hrs post dose. An overdose of sodium pentobarbital was administered via ip or iv injection after the last blood collection. For pharmacokinetic analysis, the plasma drug level data was analyzed using Phoenix® WinNonlin® (version 6.3) software to perform non compartmental modeling. The dose administered was input to the program as mg/kg.

Animals and toxicology studies of CTB-ACE2/Ang-(1–7)

Twenty-four of Sprague Dawley rats, 12 males and 12 females, were obtained from Charles River Laboratories (Hollister, CA) and assigned. General procedures for animal care and housing were accordance with previously described above. The first dose was started at the age of 8–9 weeks (males) and 9–10 weeks (females) and at 222–239 g (males) and 196–213 g (females) body weight. They were quarantined for 2 days. Oral gavage was given twice a day with 8 hours interval on Day1. Dose formulations were prepared fresh on the day of dose administration by combining lyophilized plant powder in PBS. The formulations were mixed well using magnetic stirrer for 10 to 60 min. Animals are assigned into three groups (3 males and 3 females in each group) with escalating dose range: low dose (Group-I), medium (Group-II), and high (Group-III) containing ACE2–0.08/Ang-(1–7)-1.7, ACE2–0.4/Ang-(1–7)-8.6, and ACE2–0.8/Ang-(1–7)-17 mg/kg rat body weight with negative controls (Group-0) (Suppl. Table S1). Animals were checked at least once daily for mortality and morbidity evaluations and clinical observations were recorded approximately 1–2 hr post each dose from Day 1 to the day of necropsy. Body weight was recorded on Day 1 (pre-dose) for the purpose of dose calculation and on Day 3 and Day 8. For clinical pathology evaluations on Day 3, animals were not fasted before blood collection. Blood was collected from the retro-orbital sinus of rats under 60% CO2/40% O2 anesthesia. Hematology samples were collected using K3EDTA as the anticoagulant. No anticoagulant was used for clinical chemistry samples. Necropsy was carried out on Day 8. An overdose of sodium pentobarbital was administered via intraperitoneal injection. External examination of all body orifices and an examination of all cranial, thoracic, and abdominal organs were performed, and all gross findings were recorded. No tissues were retained.

Animals and induction of experimental PH

Male SD rats (200–225 g) were obtained from Charles River Laboratories (Wilmington, MA, USA). All animals received care in accordance with the Indiana University School of Medicine Institutional Animal Care and Use Committee and adherent to the National Institutes of Health guidelines for care and use of laboratory animals under the animal welfare assurance act. Animals were allowed to acclimate for 7 days before start of oral delivery ACE2/Ang-(1–7).

Monocrotaline-induced PH (MCT-PH): PH was induced by a single subcutaneous injection of 60 mg/kg of MCT (Sigma, St. Louis, MO). Twenty-four hours later, oral delivery of CTB-ACE2 and CTB-Ang-(1–7) by gavage was started. Specifically, 50, 100 or 150 mg of CTB-ACE2 powdered leaves (0.25, 0.5, 0.75 mg of protein, correspondingly) plus 50, 100 or 150 mg of CTB-Ang-(1–7) powdered leaves (0.4, 0.8, 1.2 mg of protein, correspondingly) were mixed with PBS to generate suspensions of 100, 200 or 300 mg of plant material (50 and 50 mg, 100 and 100 mg, or 150 and 150 mg of CTB-ACE2 and CTB-Ang-(1–7), respectively). Final volumes were 3, 3 and 3.5 ml, respectively. An additional group of MCT animals (sham group) received 3.5 ml of PBS. Oral delivery was performed under isoflurane anesthesia (2% via nose cone) from Monday through Friday for a total of 4 weeks. All rats were sacrificed 4 weeks after MCT injection.

Plasma sample collection and measurement of Ang-(1–7)

Weekly injections of tail vein blood (~1 ml) were performed 5 hours after gavage. Blood was transferred to a polypropylene tube with EDTA in an ice bath. After mixing, tubes were centrifuged at 4°C for 20 min. Plasma supernatant was decanted into a new polypropylene tube and stored at −70 °C until analyzed. The quantity of circulating Ang-(1–7) was determined using an EIA kit (Peninsula Laboratories LLC, San Carlos, CA, USA), as per the manufacturer's instructions.

Assessment of cardiopulmonary hemodynamics

Echocardiography and hemodynamic assessments were performed as described previously [64–66]. Briefly, after 4 weeks of MCT treatment, RV function was evaluated by echocardiography (Vevo 2100, VisualSonics Inc., Toronto, Canada) under light isoflurane anesthesia (2%). Following echocardiography, anesthesia was maintained, and rats were intubated and mechanically ventilated (tidal volume 6 ml/kg; positive end-expiratory pressure 3 mmHg; 80 breaths/min. A 2F microtip Millar catheter (Millar, Houston, TX) was introduced through the right jugular vein into the RV for real-time measurement of RV systolic pressure (RVSP). Analyses were performed by blinded investigators.

Organ harvest and assessment of right ventricular hypertrophy (RVH)

After recording of RVSP, animals were exsanguinated. Organ harvest was performed as described previously [64–66]. Lungs were flushed with normal saline through a catheter in the pulmonary artery (PA) until clear return was observed from the left atrium. The left lung was then inflated *via* the trachea (10% buffered formalin under constant pressure of 20 mmHg). Heart and lungs were then excised. The weights of the RV free wall and left

ventricle (LV) plus septum (S) were measured in a blinded fashion to determine the Fulton index (RV/[LV+S]), a measure of RVH. The right lung and the RV inflow and outflow tracts were snap-frozen in liquid nitrogen for protein and RNA analyses; the left lung and the RV apex were immersed in 10% buffered formalin and embedded in paraffin for histological analyses (see below).

Analysis of pulmonary vascular remodeling

Lung slides were stained with Verhoeff-van Giesson (VVG) for elastin as described previously[64–66]. Pulmonary artery (PA) remodeling was examined by identifying pulmonary arterioles with a diameter of <200 μm. Total vessel area and luminal area were determined by manually outlining the outer and inner circumference of each vessel using Image J software. PA wall fraction was calculated by the formula: (total vessel area – luminal area) / (total vessel area). At least 20 vessels per rat were measured and values were averaged. Analyses were performed by a blinded investigator.

mRNA isolation and real-time RT-PCR

Total lung RNA was isolated using the RNeasy Fibrous Tissue Kit (Qiagen, Hilden, Germany) according to the manufacturer's protocol. After isolation, total RNA was transcribed into cDNA using the iScript cDNA Synthesis kit (Bio-Rad, Hercules, USA). After synthesis, RNAse free water was added to the single cDNA to a final volume of 180 μl. Quantification of gene expression was performed by quantitative real-time polymerase chain reaction on the 7500 Real-Time PCR System (Applied Biosystems, Foster City, USA) using the TaqMan™ Gene Expression Master Mix (Applied Biosystems) and specific Taq-Man probes: MAS1 - Rn00562673_s1, AGTR1a - Rn02758772_s1, IL1R1 - Rn01640664_m1, TGFb1-Rn00572010_m1, Ppia - Rn00690933_m1. Quantitative real-time polymerase chain reaction amplifications were performed in a final volume of 20 μl at 95°C for 10 minutes followed by 40 cycles with denaturation at 95°C for 15s, annealing at 60°C for 1 minute. The mRNA levels were quantified with the 7500 Real-Time PCR System Sequence Detection Software 1.3.1 in comparative quantitation mode and normalized to peptidylprolyl isomerase A (Ppia) expression levels. All samples were analyzed in duplicates and in a blinded fashion.

Statistical analyses

Data are presented as means ±SEM. Data were analyzed by one-way ANOVA followed by Newman-Keuls test for multiple comparison using GraphPad Prism 7.0 (GraphPad Software Inc, San Diego, CA). A p-value of <0.05 was considered statistically significant.

Supplementary Material

Refer to Web version on PubMed Central for supplementary material.

Acknowledgements

This research was supported by funding from NIH grant R01 HL 107904, R01 HL 109442, R01 HL 133191 to Henry Daniell. NHLBI SMARTT grant program awarded to Steven Kawut and Henry Daniell. This study was supported in part with services from the National Heart Lung and Blood Institute, National Institutes of Health,

Department of Health and Human Services, through the Science Moving TowArds Research Translation and Therapy (SMARTT) program via the following contract(s) : HHSN268201600011C (for the Coordinating Center) and HHSN268201600014C (for Pharmacology/Toxicology Center). Authors specifically thank Drs. Maria Arolfo and Dr. Hanna Ng for toxicology and pharmacokinetic studies conducted at SRI International and Drs. Cindy McClintock and Diana Severynse-Stevens for all regulatory studies conducted at RTI International.

References

[1]. Daniell H, Chan HT, and Pasoreck EK. Vaccination via Chloroplast Genetics: Affordable Protein Drugs for the Prevention and Treatment of Inherited or Infectious Human Diseases. Annu Rev Genet. 2016;50:595–618. [PubMed: 27893966]

[2]. Daniell H, Kulis M, Herzog RW Plant cell-made protein antigens for induction of Oral tolerance, Biotechnol Adv 2019, published online

[3]. Kwon KC, and Daniell H. Oral Delivery of Protein Drugs Bioencapsulated in Plant Cells. Mol. Ther 2016;24:1342–50. [PubMed: 27378236]

[4]. Boyhan D, and Daniell H. Low-cost production of proinsulin in tobacco and lettuce chloroplasts for injectable or oral delivery of functional insulin and C-peptide. Plant Biotechnol J. 2011; 9:585–98. [PubMed: 21143365]

[5]. Kwon KC, Nityanandam R, New JS, and Daniell H. Oral delivery of bioencapsulated exendin-4 expressed in chloroplasts lowers blood glucose level in mice and stimulates insulin secretion in beta-TC6 cells. Plant Biotechnol J. 2013;11:77–86. [PubMed: 23078126]

[6]. Shenoy V, Kwon KC, Rathinasabapathy A, Lin S, Jin G, Song C, et al. Oral delivery of Angiotensin-converting enzyme 2 and Angiotensin-(1–7) bioencapsulated in plant cells attenuates pulmonary hypertension. Hypertension. 2014;64:1248–59. [PubMed: 25225206]

[7]. Kohli N, Westerveld DR, Ayache AC, Verma A, Shil P, Prasad T, et al. Oral delivery of bioencapsulated proteins across blood-brain and blood-retinal barriers. Mol Ther. 2014; 22:535–46. [PubMed: 24281246]

[8]. Shil PK, Kwon KC, Zhu P, Verma A, Daniell H, and Li Q. Oral delivery of ACE2/Ang-(1–7) bioencapsulated in plant cells protects against experimental uveitis and autoimmune uveoretinitis. Mol Ther. 2014; 22:2069–82. [PubMed: 25228068]

[9]. Verma D, Moghimi B, LoDuca PA, Singh HD, Hoffman BE, Herzog RW, et al. Oral delivery of bioencapsulated coagulation factor IX prevents inhibitor formation and fatal anaphylaxis in hemophilia B mice. PNAS. 2010; 107:7101–6. [PubMed: 20351275]

[10]. Sherman A, Su J, Lin S, Wang X, Herzog RW, and Daniell H. Suppression of inhibitor formation against FVIII in a murine model of hemophilia A by oral delivery of antigens bioencapsulated in plant cells. Blood. 2014; 124:1659–68. [PubMed: 24825864]

[11]. Kwon KC, Sherman A, Chang WJ, Kamesh A, Biswas M, Herzog RW, et al. Expression and assembly of largest foreign protein in chloroplasts: oral delivery of human FVIII made in lettuce chloroplasts robustly suppresses inhibitor formation in haemophilia A mice. Plant Biotechnol J. 2017; 16:1148–60. [PubMed: 29106782]

[12]. Herzog RW, Nichols TC, Su J, Zhang B, Sherman A, Merricks EP, et al. Oral Tolerance Induction in Hemophilia B Dogs Fed with Transplastomic Lettuce. Molecular Therapy. 2017; 25:512–22. [PubMed: 28153098]

[13]. Su J, Zhu LQ, Sherman A, Wang XM, Lin SN, Kamesh A, et al. Low cost industrial production of coagulation factor IX bioencapsulated in lettuce cells for oral tolerance induction in hemophilia B. Biomaterials. 2015; 70:84–93. [PubMed: 26302233]

[14]. Rabinovitch M Molecular pathogenesis of pulmonary arterial hypertension. J. Clin. Investig 2012; 122:4306–13. [PubMed: 23202738]

[15]. Humbert M, Sitbon O, Chaouat A, Bertocchi M, Habib G, Gressin V, et al. Survival in patients with idiopathic, familial, and anorexigen-associated pulmonary arterial hypertension in the modern management era. Circulation. 2010; 122:156–63. [PubMed: 20585011]

[16]. Stacher E, Graham BB, Hunt JM, Gandjeva A, Groshong SD, McLaughlin VV, et al. Modern age pathology of pulmonary arterial hypertension. Am. J. Respir. Crit. Care Med. 2012; 186:261–72. [PubMed: 22679007]

[17]. Newman JH, Rich S, Abman SH, Alexander JH, Barnard J, Beck GJ, et al. Enhancing Insights into Pulmonary Vascular Disease through a Precision Medicine Approach. A Joint NHLBI-Cardiovascular Medical Research and Education Fund Workshop Report. Am. J. Respir. Crit. Care Med. 2017; 195:1661–70. [PubMed: 28430547]

[18]. Sutendra G, and Michelakis ED. Pulmonary arterial hypertension: challenges in translational research and a vision for change. Sci. Transl. Med 2013; 5:208sr5. [PubMed: 24154604]

[19]. Sitbon O, Manes A, Jais X, Pallazini M, Humbert M, Presotto L, et al. Rapid switch from intravenous epoprostenol to intravenous treprostinil in patients with pulmonary arterial hypertension. J. Cardiovasc. Pharmacol 2007; 49:1–5. [PubMed: 17261956]

[20]. Putnam K, Shoemaker R, Yiannikouris F, and Cassis LA. The renin-angiotensin system: a target of and contributor to dyslipidemias, altered glucose homeostasis, and hypertension of the metabolic syndrome. Am. J. Physiol. Heart Circ. Physiol 2012; 302:H1219–H30. [PubMed: 22227126]

[21]. Bader M ACE2, angiotensin-(1–7), and Mas: the other side of the coin. Pflugers Archiv-European Journal of Physiology. 2013; 465:79–85. [PubMed: 23463883]

[22]. de Man FS, Handoko ML, Guignabert C, Bogaard HJ, and Vonk-Noordegraaf A. Neurohormonal axis in patients with pulmonary arterial hypertension: friend or foe? Am. J. Respir. Crit. Care Med. 2013; 187:14–9. [PubMed: 23144327]

[23]. Maron BA, and Leopold JA. Emerging Concepts in the Molecular Basis of Pulmonary Arterial Hypertension: Part II: Neurohormonal Signaling Contributes to the Pulmonary Vascular and Right Ventricular Pathophenotype of Pulmonary Arterial Hypertension. Circulation. 2015; 131:2079–91. [PubMed: 26056345]

[24]. Samokhin AO, Stephens T, Wertheim BM, Wang RS, Vargas SO, Yung LM, et al. NEDD9 targets COL3A1 to promote endothelial fibrosis and pulmonary arterial hypertension. Sci. Transl. Med2018; 10:eaap7294. [PubMed: 29899023]

[25]. de Man FS, Tu L, Handoko ML, Rain S, Ruiter G, Francois C, et al. Dysregulated renin-angiotensin-aldosterone system contributes to pulmonary arterial hypertension. Am. J. Respir. Crit. Care Med. 2012; 186:780–9. [PubMed: 22859525]

[26]. Maron BA, Zhang YY, White K, Chan SY, Handy DE, Mahoney CE, et al. Aldosterone inactivates the endothelin-B receptor via a cysteinyl thiol redox switch to decrease pulmonary endothelial nitric oxide levels and modulate pulmonary arterial hypertension. Circulation. 2012; 126:963–74. [PubMed: 22787113]

[27]. Maron BA, Opotowsky AR, Landzberg MJ, Loscalzo J, Waxman AB, and Leopold JA. Plasma aldosterone levels are elevated in patients with pulmonary arterial hypertension in the absence of left ventricular heart failure: a pilot study. Eur. J. Heart Fail. 2013;15:277–83. [PubMed: 23111998]

[28]. Maron BA, Waxman AB, Opotowsky AR, Gillies H, Blair C, Aghamohammadzadeh R, et al. Effectiveness of spironolactone plus ambrisentan for treatment of pulmonary arterial hypertension (from the [ARIES] study 1 and 2 trials). Am J Cardiol. 2013; 112:720–725. [PubMed: 23751938]

[29]. Aghamohammadzadeh R, Zhang YY, Stephens TE, Arons E, Zaman P, Polach KJ, et al. Up-regulation of the mammalian target of rapamycin complex 1 subunit Raptor by aldosterone induces abnormal pulmonary artery smooth muscle cell survival patterns to promote pulmonary arterial hypertension. FASEB J. 2016; 30:2511–27. [PubMed: 27006450]

[30]. Boehm M, Arnold N, Braithwaite A, Pickworth J, Lu C, Novoyatleva T, et al. Eplerenone attenuates pathological pulmonary vascular rather than right ventricular remodeling in pulmonary arterial hypertension. BMC Pulm Med. 2018; 18:41. [PubMed: 29499691]

[31]. Ferreira AJ, Shenoy V, Yamazato Y, Sriramula S, Francis J, Yuan L, et al. Evidence for angiotensin-converting enzyme 2 as a therapeutic target for the prevention of pulmonary hypertension. Am. J. Respir. Crit. Care Med. 2009; 179:1048–54. [PubMed: 19246717]

[32]. Shenoy V, Ferreira AJ, Qi Y, Fraga-Silva RA, Diez-Freire C, Dooies A, et al. The angiotensin-converting enzyme 2/angiogenesis-(1–7)/Mas axis confers cardiopulmonary protection against lung fibrosis and pulmonary hypertension. Am. J. Respir. Crit. Care Med. 2010; 182:1065–1072. [PubMed: 20581171]

[33]. Hampl V, Herget J, Bibova J, Banasova A, Huskova Z, Vanourkova Z, et al. Intrapulmonary activation of the angiotensin-converting enzyme type 2/angiotensin 1–7/G-protein-coupled Mas receptor axis attenuates pulmonary hypertension in Ren-2 transgenic rats exposed to chronic hypoxia. Physiol Res. 2015; 64:25–38. [PubMed: 25194138]

[34]. Rathinasabapathy A, Bryant AJ, Suzuki T, Moore C, Shay S, Gladson S, et al. rhACE2 Therapy Modifies Bleomycin-Induced Pulmonary Hypertension via Rescue of Vascular Remodeling. Front Physiol. 2018; 9:271. [PubMed: 29731719]

[35]. Johnson JA, West J, Maynard KB, and Hemnes AR. ACE2 improves right ventricular function in a pressure overload model. PLoS One. 2011; 6:e20828. [PubMed: 21695173]

[36]. Breitling S, Krauszman A, Parihar R, Walther T, Friedberg MK, and Kuebler WM. Dose-dependent, therapeutic potential of angiotensin-(1–7) for the treatment of pulmonary arterial hypertension. Pulm. Circ 2015; 5:649–657. [PubMed: 26697172]

[37]. Kwon KC, Chan HT, Leon IR, Williams-Carrier R, Barkan A, and Daniell H. Codon Optimization to Enhance Expression Yields Insights into Chloroplast Translation. Plant Physiol. 2016; 172:62–77. [PubMed: 27465114]

[38]. Duckert P, Brunak S, and Blom N. Prediction of proprotein convertase cleavage sites. Protein Eng. Des. Sel 2004; 17:107–12. [PubMed: 14985543]

[39]. Park J, Yan G, Kwon K-C, Liu M, Gonnella PA, Yang S, and Daniell H. Oral delivery of novel human IGF-1 bioencapsulated in lettuce cells promotes musculoskeletal cell proliferation, differentiation and diabetic fracture healing. Biomaterials 2019: 119591. [PubMed: 31870566]

[40]. Yung LM, Nikolic I, Paskin-Flerlage SD, Pearsall RS, Kumar R, and Yu PB. A Selective Transforming Growth Factor-beta Ligand Trap Attenuates Pulmonary Hypertension. Am. J. Respir. Crit. Care Med. 2016; 194:1140–51. [PubMed: 27115515]

[41]. Zaiman AL, Podowski M, Medicherla S, Gordy K, Xu F, Zhen L, et al. Role of the TGF-beta/Alk5 signaling pathway in monocrotaline-induced pulmonary hypertension. Am. J. Respir. Crit. Care Med. 2008; 177:896–905. [PubMed: 18202349]

[42]. De Cosa B, Moar W, Lee SB, Miller M, and Daniell H. Overexpression of the Bt cry2Aa2 operon in chloroplasts leads to formation of insecticidal crystals. Nat. Biotechnol 2001; 19:71–74. [PubMed: 11135556]

[43]. Ruhlman T, Verma D, Samson N, and Daniell H. The Role of Heterologous Chloroplast Sequence Elements in Transgene Integration and Expression. Plant Physiol. 2010; 152:2088–104. [PubMed: 20130101]

[44]. Jin SX, and Daniell H. The Engineered Chloroplast Genome Just Got Smarter. Trends Plant Sci. 2015; 20:622–640. [PubMed: 26440432]

[45]. Daniell H, Ribeiro T, Lin S, Saha P, McMichael C, Chowdhary R, Agarwal A. Validation of leaf and microbial pectinases: commercial launching of a new platform technology, Plant Biotechnol. J 2019; 17: 1154–1166. [PubMed: 30963657]

[46]. Kumari U, Singh R, Ray T, Rana S, Saha P, Malhotra K, Daniell H. Validation of leaf enzymes in the detergent and textile industries: launching of a new platform technology, Plant Biotechnol. J 2019; 17: 1167–1182. [PubMed: 30963679]

[47]. Kode V, Mudd EA, Iamtham S, Day A. Isolation of precise plastid deletion mutants by homology-based excision: a resource for site-directed mutagenesis, multi-gene changes and high-throughput plastid transformation. Plant J. 2006; 46:901–909. [PubMed: 16709203]

[48]. Iamtham S, Day A. Removal of antibiotic resistance genes from transgenic tobacco plastids, Nat. Biotechnol 2000; 18: 1172–1176. [PubMed: 11062436]

[49]. Daniell H, Lin CS, Yu M, and Chang WJ. Chloroplast genomes: diversity, evolution, and applications in genetic engineering. Genome Biol. 2016;17:134. [PubMed: 27339192]

[50]. Tipnis SR, Hooper NM, Hyde R, Karran E, Christie G, and Turner AJ. A human homolog of angiotensin-converting enzyme. Cloning and functional expression as a captopril-insensitive carboxypeptidase. J Biol Chem. 2000; 275: 33238–33243. [PubMed: 10924499]

[51]. Khan A, Benthin C, Zeno B, et al. A pilot clinical trial of recombinant human angiotensin-converting enzyme 2 in acute respiratory distress syndrome. Crit Care. 2017; 21:234. [PubMed: 28877748]

[52]. Patel VB, Clarke N, Wang Z, Fan D, Parajuli N, Basu R, Putko B, Kassiri Z, Turner AJ, Oudit GY.Angiotensin II induced proteolytic cleavage of myocardial ACE2 is mediated by TACE/ADAM-17: a positive feedback mechanism in the RAS.J Mol Cell Cardiol. 2014; 66:167–176. [PubMed: 24332999]

[53]. Wysocki J, Ye M, Khattab AM et al. Angiotensin-converting enzyme 2 amplification limited to the circulation does not protect mice from development of diabetic nephropathy. Kidney Int. 2017; 91: 1336–1346 [PubMed: 27927599]

[54]. Zou Y, Xue W, Luo G, Deng Z, Qin P, et al. 1,520 reference genomes from cultivated human gut bacteria enable functional microbiome analyses. Nat Biotechnol. 2019; 37:179–185. [PubMed: 30718868]

[55]. Angelakis E, Armougom F, Carriere F, Bachar D, Laugier R, et al. A Metagenomic Investigation of the Duodenal Microbiota Reveals Links with Obesity. PLoS One. 2015;10:e0137784. [PubMed: 26356733]

[56]. Flint HJ, Scott KP, Duncan SH, Louis P, Forano E. Microbial degradation of complex carbohydrates in the gut. Gut microbes, 2012, 3(4), 289–306. [PubMed: 22572875]

[57]. Humbert M, Monti G, Brenot F, Sitbon O, Portier A, Grangeot-Keros L, et al. Increased interleukin-1 and interleukin-6 serum concentrations in severe primary pulmonary hypertension. Am. J. Respir. Crit. Care Med. 1995; 151:1628–31. [PubMed: 7735624]

[58]. Freeman EJ, Chisolm GM, Ferrario CM, and Tallant EA. Angiotensin-(1–7) inhibits vascular smooth muscle cell growth. Hypertension. 1996; 28:104–108. [PubMed: 8675248]

[59]. Gallagher PE, and Tallant EA. Inhibition of human lung cancer cell growth by angiotensin-(1–7). Carcinogenesis. 2004; 25:2045–52. [PubMed: 15284177]

[60]. Xiao YH, Kwon KC, Hoffman BE, Kamesh A, Jones NT, Herzog RW, et al. Low cost delivery of proteins bioencapsulated in plant cells to human non-immune or immune modulatory cells. Biomaterials. 2016; 80:68–79. [PubMed: 26706477]

[61]. Hemnes AR, Rathinasabapathy A, Austin EA, Brittain EL, Carrier EJ, Chen X, et al. A potential therapeutic role for angiotensin-converting enzyme 2 in human pulmonary arterial hypertension. Eur. Respir. J 2018; 51:1702638. [PubMed: 29903860]

[62]. Haschke M, Schuster M, Poglitsch M, Loibner H, Salzberg M, Bruggisser M, et al. Pharmacokinetics and Pharmacodynamics of Recombinant Human Angiotensin-Converting Enzyme 2 in Healthy Human Subjects. Clin Pharmacokinet 2013; 52:783–792. [PubMed: 23681967]

[63]. Verma D, Samson NP, Koya V, and Daniell H. A protocol for expression of foreign genes in chloroplasts. Nat Protoc. 2008; 3:739–758. [PubMed: 18388956]

[64]. Frump AL, Goss KN, Vayl A, Albrecht M, Fisher A, Tursunova R, et al. Estradiol improves right ventricular function in rats with severe angioproliferative pulmonary hypertension: effects of endogenous and exogenous sex hormones. Am J Physiol Lung Cell Mol Physiol. 2015; 308:L873–890. [PubMed: 25713318]

[65]. Lahm T, Albrecht M, Fisher AJ, Selej M, Patel NG, Brown JA, et al. 17beta-Estradiol attenuates hypoxic pulmonary hypertension via estrogen receptor-mediated effects. Am. J. Respir. Crit. Care Med. 2012; 185:965–980. [PubMed: 22383500]

[66]. Lahm T, Frump AL, Albrecht ME, Fisher AJ, Cook TG, Jones TJ, et al. 17beta-Estradiol mediates superior adaptation of right ventricular function to acute strenuous exercise in female rats with severe pulmonary hypertension. Am J Physiol Lung Cell Mol Physiol. 2016; 311:L375–388. [PubMed: 27288487]

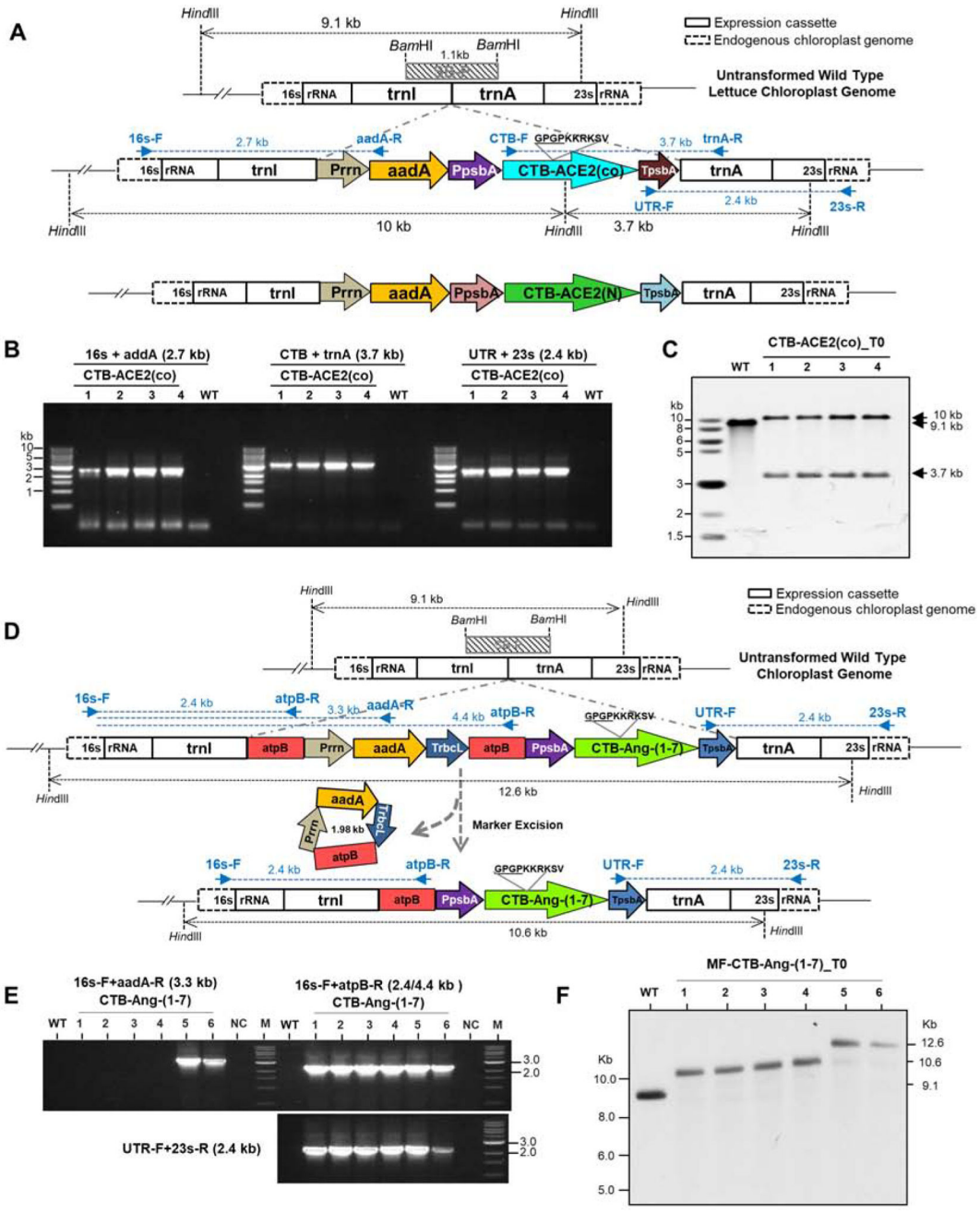

Fig. 1. Creation of transplastomic lettuce lines with stable integration of CTB-ACE2 and CTB-Ang-(1–7).

(A) Schematic diagram of chloroplast transformation vector map containing CTB-ACE2 expression cassette. 16s and 23s rRNA, 16s and 23s ribosomal RNA; trnI, isoleucyl-tRNA; trnA, alanyl-tRNA; Prrn, rRNA operon promoter; CTB-ACE2(co), codon optimized angiotensin converting enzyme2 with CTB (Cholera non-Toxin B subunit) fusion; TpsbA, 3 ´-UTR of psbA. Blue arrows show PCR primers annealing sites with expected amplified sizes. Diagram of native ACE2 in tobacco expression cassette is located at the bottom. SB-P, Southern blot probe. **(B)** Genomic DNA PCR amplification with three sets of primers. **(C)** Southern blot analysis of CTB-ACE2 transplastomic lines. Expected sizes are indicated in

black arrows. **(B-C)** Lanes 1 to 4, individual lettuce transplastomic lines; WT, untransformed wild type. **(D)** Schematic diagram of CTB-Ang-(1–7) gene in expression cassette of lettuce chloroplast marker-free vector and process of marker excision. Ang-(1–7), Angiotensin-(1–7). SB-P, Southern blot probe. **(E)** PCR analysis with three sets of primers. WT, untransformed wild type; M; DNA standard, lanes 1 to 6, transplastomic lines. **(F)** Southern blot analysis for MF-CTB-Ang-(1–7) transplastomic lines. WT, untransformed wild type; lanes 1 to 6, transplastomic T0 seedlings. Expected sizes are indicated in arrows.

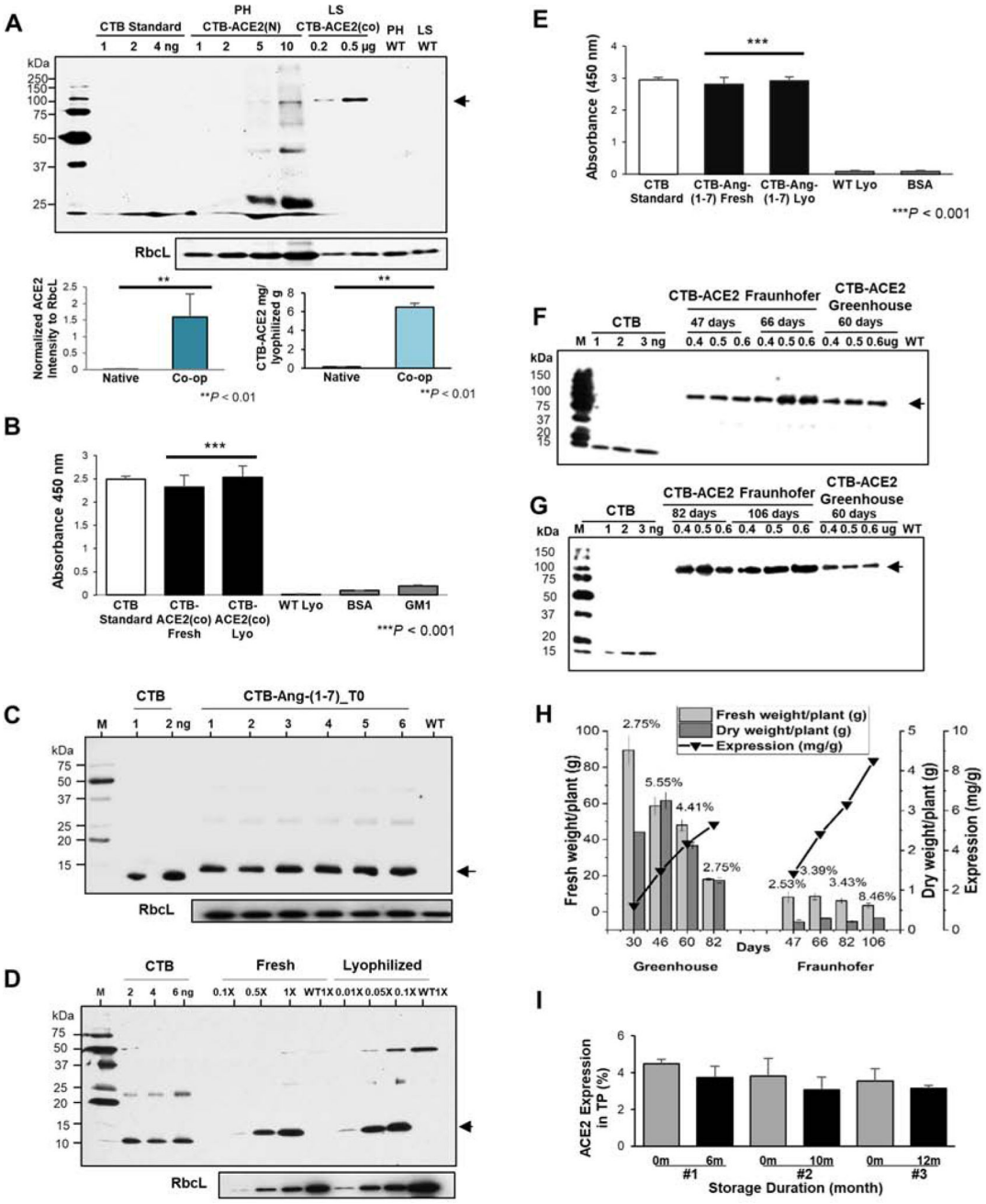

Fig. 2. Characterizations of CTB-ACE2(co) and CTB-Ang-(1–7) expression, stability, storage, and clinical grade production.

(A) Immunoblot analysis between native ACE2(N) and codon optimized ACE2(co). The bottom graph visualizes the mean ± SD of normalized ACE2 intensities to RbcL (loading controls) (bottom). **P-value < 0.01 vs. Native. PH, tobacco Petit Havana; LS, lettuce; WT, untransformed wild type; N, native sequence; CO, codon-optimized sequence. **(C)** Western blot of CTB-Ang-(1–7) T0 generation. Lanes #1 to 6, individual plant. **(D)** Western blot of CTB-Ang-(1–7) in equal amount of fresh and lyophilized plant cells (1X). **(C-D)** WT, untransformed wild type lettuce, M, protein standard; CTB, cholera non-toxic B subunit;

Lyo, lyophilized lettuce. RbcL was used as loading controls. GM1 ELISA assay of **(B)** CTB-ACE2 and **(E)** CTB-Ang-(1–7) pentamer. WT, untransformed wild type; Lyo, lyophilized lettuce. Data are expressed as the mean ± SD. ***P-value < 0.001 vs. WT. The data obtained from two independent biological repeats run in triplicates. **(F)** Western blot analysis of ACE2 accumulation in transplastomic lettuce plants harvested from Fraunhofer hydroponically (FH) and Greenhouse (GH) with different times **(F and G)**. Western blot was performed for different ages ranged from 46 days and 66 days for FH and 46 days for GH **(F)**, 82 days and 106 days for FH and 60 days for GH **(G)**; The amount of TP loaded is given above the respective lane in g. The arrows indicate the 100 kDa Ace2. M: spectra multicolour broad range protein ladder (Thermo Scientific, molecular weight of the marker bands indicated in kDa). **(H)** Determination of fresh weight, dry weight, ACE2 expression, and ACE2 yield per plant with different ages between Greenhouse and Fraunhofer. Plant ages are relative to the date of germination. Fresh and dry weight per plant are calculated by normalization of total fresh and dry weight to total number of plants grown in Greenhouse (16) and Fraunhofer (400). The percentage of water content (the ratio of dry material / fresh material) are shown on the top of column. **(I)** Stability of CTB-ACE2 after long-term storage. #1 to #3, individual lettuce CTB-ACE2(co) transplastomic lines. Data are expressed as the mean ± SD.

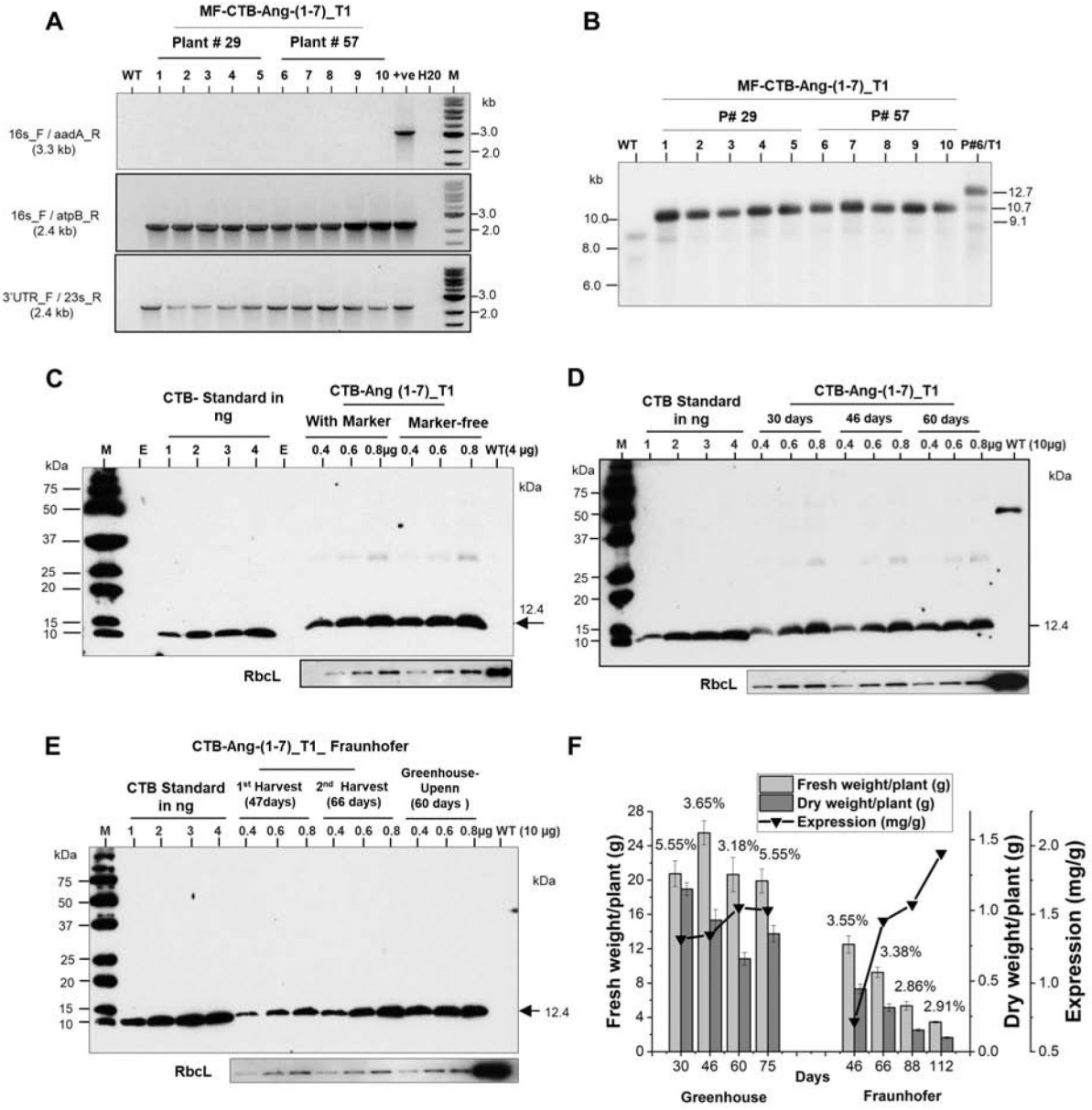

Fig. 3. Characterizations of CTB-Ang-(1–7) marker-free plants and clinical grade production

(A) T0 seeds of plant lines #29 and 57 were grown on ½ MS0 medium without spectinomycin. After few weeks, genomic DNA was evaluated by PCR using the three sets of primers. Lane #1 WT, untransformed wild type; lanes # 2 to 6 plant # 29, Lanes # 7 to 11 plant #57; Lane# 12 positive control; lane # 13 PCR mix with H20; Lane # 14 M; 1 kb ladder **(B)** gDNA digested with HindIII. Lane 1, 1 kb ladder DNA; Lane 2, UT, untransformed; Lanes 3–7 DNA from marker-free seedlings of T0 plant#29; Lane 8–12 DNA from marker-free seedlings of T0 plant#57; Lane 13 T1 plant contacting the aadA gene. The position of the expected sizes of fragment is untransformed 9.1-kb, selectable marker-free is 10.7-kb, with selectable marker is 12.7-kb are indicated with arrows. Western blot of CTB-Ang-(1–7) in lettuce plants with or without the selectable marker gene **(C). (D)** The immunoblot assay of CTB-Ang-(1–7) expressed lettuce lyophilized leaves harvested

after 30, 46 days or 60 days of plants grown in the greenhouse. **(E)** The immunoblot assay of CTB-Ang-(1–7) expressed in lettuce lyophilized leaves harvested at 47 days, 66 days from the plants grown in hydroponic system at Fraunhofer. 0.4 μg, 0.6μg,0.8μg of TLP Per lane was loaded and probed with anti-CTB rabbit polyclonal antibody. **(F)** Determination of fresh weight, dry weight, Ang1–7 expression and yield per plant of different ages grown at the Greenhouse or Fraunhofer. Fresh and dry weight per plant are calculated by normalization of total fresh and dry weight to total number of plants grown in Greenhouse (60) and Fraunhofer (800). The percentage of water content (the ratio of dry material / fresh material) are shown on the top of column.

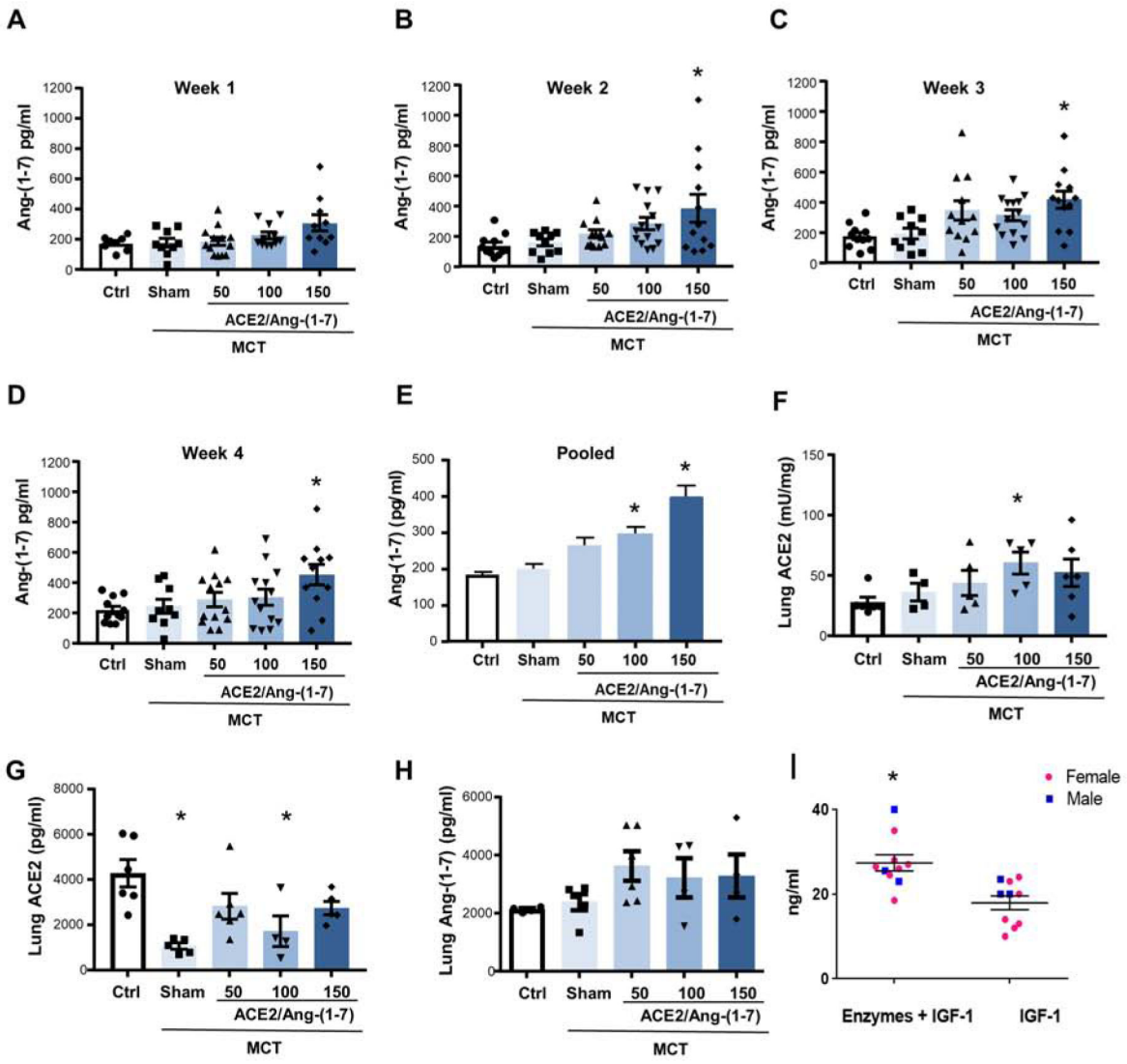

Fig. 4. Pharmacokinetic Study of CTB-ACE2/Ang-(1–7) following oral dose administrations.

Increases of Ang-(1–7) plasma levels in rats with monocrotaline-induced pulmonary hypertension by combinational feeding with bioencapsulated CTB-ACE2 and CTB-Ang-(1–7). CTB-ACE2 (50, 100 or 150 mg of plant material; containing 0.4, 0.8 and 1.2 mg of ACE2 protein) and CTB-Ang-(1–7) (50, 100 or 150 mg of plant material; containing 0.25, 0.5 and 0.7 mg of Ang-(1–7) protein) were gavaged daily. Animals in sham group were gavaged with PBS only. Levels were measured once a week 5h after gavage. **(A-D)** Absolute Ang-(1–7) plasma levels for each week (1 to 4). Each data point represents one animal. **(E)** Pooled Ang-(1–7) plasma levels (combined data of week 1 to 4) are shown. **(F-H)** Lung ACE2 activity and quantity as well as lung Ang-(1–7) levels. Error bars or values represent ± SEM. #p < 0.05 vs. MCT groups by one-way ANOVA and post-hoc Newman-Keuls test. Ctrl = untreated control; MCT = monocrotaline. **(I)** C57BL/6J mice were gavaged with the enzymes mannanase, pectinate lyase, endoglucanase and exoglucanase (5 mg plant powder/enzyme) and one hour later gavaged with PTD-Pro-IGF-1 (5ug IGF-1/20mg plant powder). Controls were gavaged with PBS followed by PTD-Pro IGF-1. *p=0.009.

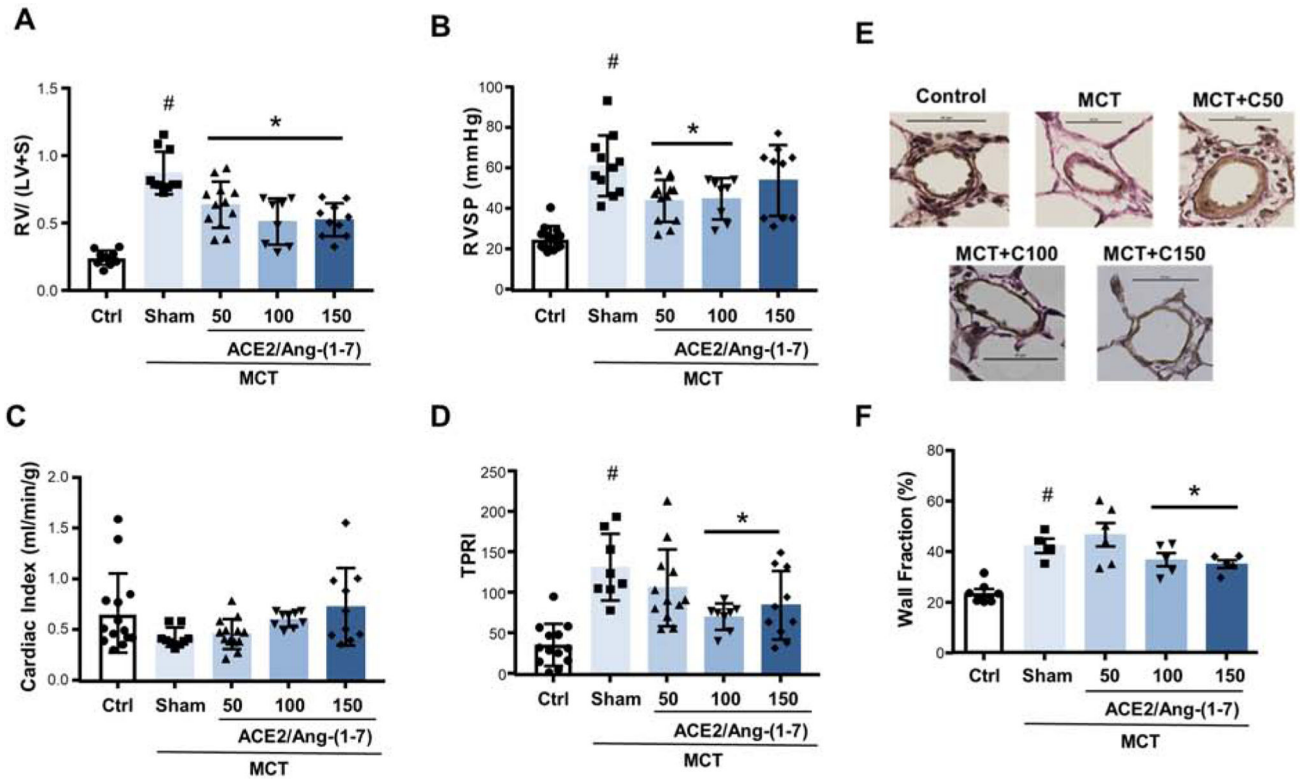

Fig. 5. Attenuation of experimental pulmonary hypertension by combinational feeding with bioencapsulated CTB-ACE2 and CTB-Ang-(1–7).

Effects of bioencapsulated CTB-ACE2 and CTB-Ang-(1–7) on **(A)** Fulton index (a marker of RV hypertrophy; calculated as the ratio of the right ventricle [RV] weight to the weight of the left ventricle plus septum [LV+S], **(B)** RV systolic pressure (RVSP), **(C)** cardiac index (CI; determined echocardiographically), **(D)** total pulmonary resistance index (TPRI [a marker of RV afterload]; calculated as ratio of RVSP and CI), and **(E)** pulmonary vascular remodeling (quantified as percent wall area). Representative photomicrographs of peripheral pulmonary arteries (Verhoeff-van Giesson stain) are shown on the bottom of **(E)**; quantification of percent wall area is shown on right. CTB-ACE2, CTB-Ang-(1–7) or PBS were administered as outlined in Figure 4. Each data point represents one animal. Values are means ± SEM. #p <0.05 vs. control, *p <0.05 vs. sham by one-way ANOVA and post-hoc Newman-Keuls test. Ctrl = untreated control; MCT = monocrotaline.

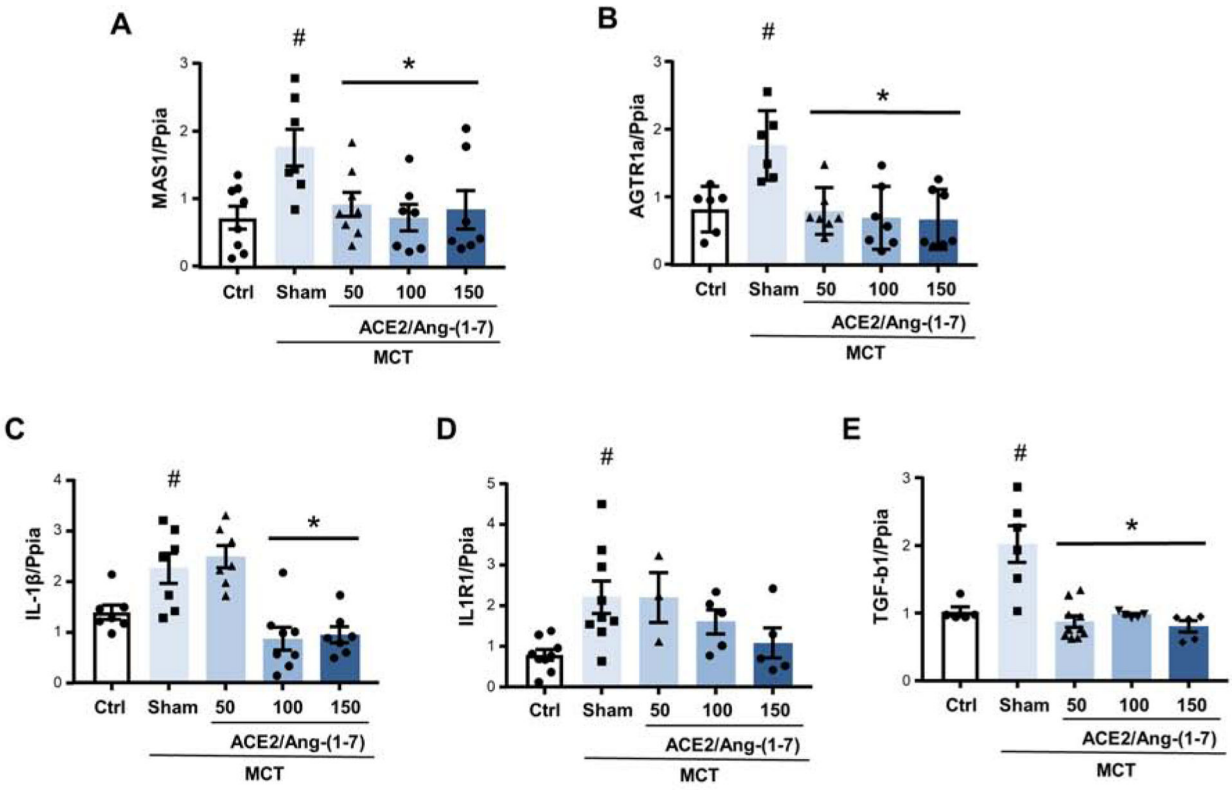

Fig. 6. Attenuation of pulmonary hypertension-induced alterations in expression of genes implicated in PAH pathogenesis by combinational feeding with bioencapsulated CTB-ACE2 and CTB-Ang-(1–7)

(A) MAS1, **(B)** AGTR1, **(C)** IL-1β, **(D)** IL1R1, and **(E)** TGF-β1 mRNA levels were determined by real time RT-PCR and are expressed as fold change Ct vs. peptidylprolyl isomerase A (Ppia) expression levels. CTB-ACE2, CTB-Ang-(1–7) or PBS were administered as outlined in Figure 4. Each data point represents one animal. Values are means ± SEM. #p <0.05 vs. control, *p <0.05 vs. sham by one-way ANOVA and post-hoc Newman-Keuls test. Ctrl = untreated control; MCT = monocrotaline.